



Stable isotope record of *Triceratops* from a mass accumulation (Lance Formation, Wyoming, USA) provides insights into *Triceratops* behaviour and ecology

Jimmy de Rooij^{a,d,*}, Jeroen H.J.L. van der Lubbe^b, Suzan Verdegaaal^b, Megan Hulscher^c, Daphne Tooms^b, Pim Kaskes^{a,b,e}, Oeki Verhage^{a,b}, Leonie Portanger^{a,b}, Anne S. Schulp^{a,d}

^a Naturalis Biodiversity Center, Darwinweg 2, 2333 CR Leiden, the Netherlands

^b Department of Earth Sciences, Faculty of Science, Vrije Universiteit, De Boelelaan 1085, 1081 HV Amsterdam, the Netherlands

^c Institute of Biology, Faculty of Science, Leiden University, Sylviusweg 72, 2333 BE Leiden, the Netherlands

^d Faculty of Geosciences, Utrecht University, Princetonlaan 8A, 3584 CB Utrecht, the Netherlands

^e Analytical, Environmental & Geo-Chemistry (AMGC) Research Unit, Vrije Universiteit Brussel, Pleinlaan 2, B-1050 Brussels, Belgium

ARTICLE INFO

Editor: H Falcon-Lang

Keywords:

Stable isotopes
Seasonality
Diagenesis
Niche partitioning
Bioapatite

ABSTRACT

Our understanding of Late Cretaceous dinosaur ecosystems from North America has considerably improved through stable isotope analyses on fossil bones and teeth. Oxygen and carbon stable isotopic compositions of structurally-bound carbonate in these fossil apatites are commonly used to infer variations of ingested water and food sources, which are in turn related to environmental and climatic conditions. Incremental isotopic records potentially provide insights into seasonality and migratory behaviour. So far, these reconstructions are based on vertebrate remains from spatiotemporally diverse datasets. Here, we present oxygen ($\delta^{18}\text{O}$) and carbon ($\delta^{13}\text{C}$) isotopic records from a large, spatially and temporally well-constrained, *Triceratops* bonebed from the Upper Maastrichtian Lance Formation (eastern Wyoming, USA). These isotopic compositions allow to elucidate the palaeoecology of these large herbivores and their ecosystem in detail, as well as their habitat use, diet and possible migration. The $\delta^{18}\text{O}$ signature from incrementally sampled *Triceratops* teeth reveal relatively low intra-tooth variation (average 1.3 ‰), comparable to contemporaneous dinosaur species as well as modern herbivorous mammals. Average $\delta^{13}\text{C}$ values (−5.4 ‰) are somewhat higher than for modern C3 plant grazers, and hint towards complex interactions during carbon uptake by non-avian herbivorous dinosaurs. Calculated $\delta^{18}\text{O}$ of drinking water (−14.8 ‰) combined with the local sedimentology of fine-grained siliciclastic deposits with high total organic and low carbonate contents strongly suggest a freshwater environment. Additionally, the combined average $\delta^{18}\text{O}$ and $\delta^{13}\text{C}$ *Triceratops* isotope signatures indicate a living environment intermediate between inland forests and coastal floodplains, expanding on earlier theories of ornithischian niche partitioning. Our robust dataset provides meaningful tests of habitat and palaeoecological hypotheses for *Triceratops*, and highlights the application of spatiotemporally well-constrained fossil remains.

1. Introduction

The iconic ceratopsian dinosaur *Triceratops* is known for its adorned skull and relatively large body size (Goodwin et al., 2006; Horner and Goodwin, 2006). While the *Triceratops* fossil record encompasses numerous well-preserved specimens, especially skulls of different ontogenetic age (Goodwin et al., 2006; Horner and Goodwin, 2006), little focus has been on behavioural and ecological topics including growth, feeding, gregariousness/herding and migration (Farke et al.,

2009; Mathews et al., 2009; Erickson et al., 2015; Illies and Fowler, 2020). The discovery of a large well-constrained bonebed (Kaskes et al., 2016, 2019) preserving the remains of at least five *Triceratops* individuals of varying ontogenetic age (sensu Horner and Goodwin, 2006; Bastiaans et al., 2016) in Wyoming, USA, presents a unique opportunity to elucidate ceratopsian palaeobiology and -ecology. Moreover, the bonebed is characterized by a relatively large proportion of postcranial material, while, in contrast, *Triceratops* finds are normally mainly restricted to the more robust cranial parts (Goodwin et al., 2010; Brown

* Corresponding author at: Naturalis Biodiversity Center, Darwinweg 2, 2333 CR Leiden, the Netherlands.

E-mail addresses: jimmy.derooij@naturalis.nl (J. de Rooij), h.j.l.vander.lubbe@vu.nl (J.H.J.L. van der Lubbe), anne.schulp@naturalis.nl (A.S. Schulp).

<https://doi.org/10.1016/j.palaeo.2022.111274>

Received 12 April 2022; Received in revised form 10 October 2022; Accepted 10 October 2022

Available online 13 October 2022

0031-0182/© 2022 The Authors. Published by Elsevier B.V. This is an open access article under the CC BY license (<http://creativecommons.org/licenses/by/4.0/>).

et al., 2022). Associated fauna include lepisosteids and aquatic reptiles such as *Brachychampsia* and *Champsosaurus*.

Stable isotopes analyses of bioapatite tissues from modern ecosystems provide information on the behaviour, metabolism, and ecology of extant species (Layman et al., 2012; Hobson and Wassenaar, 2018). Similarly, stable isotopes in fossil bioapatite have improved our understanding of ancient ecosystems, where they provide important insights into the biology and ecology of the Late Cretaceous dinosaur fauna of North America (Stanton Thomas and Carlson, 2004; Fricke and Pearson, 2008; Fricke et al., 2009; Terrill et al., 2020; Burgener et al., 2021). These topics – ranging from ecosystem to individual scale – include niche partitioning and habitat preference (Stanton Thomas and Carlson, 2004; Fricke and Pearson, 2008; Fricke et al., 2009; Cullen et al., 2022), community and food web structure (Ostrom et al., 1993; Cullen et al., 2022), climate (Amiot et al., 2004; Straight et al., 2004), migration (Fricke et al., 2009; Terrill et al., 2020), provenance of fossil material (Dufour et al., 2007; Tütken et al., 2011), (ontogenetic) shifts in feeding habits (Frederickson et al., 2020) and body temperature and metabolism (Barrick, 1998; Amiot et al., 2006; Eagle et al., 2011). Until now, stable isotope research on dinosaurs was heavily skewed towards theropods and hadrosaurs (Fricke and Rogers, 2000; Straight et al., 2004; Fricke et al., 2009; Goedert et al., 2016; Terrill et al., 2020) while many other taxa including ceratopsians have received relatively little attention.

Here, we present oxygen and carbon stable isotope analyses on the diverse fossil content of the so-called ‘Darnell *Triceratops* Bonebed’ (DTB). Isotope analysis of different bioapatite tissues (i.e., bone, dentine, enamel(oid)) among the different fossil taxa helps to evaluate the degree of (geochemical) preservation and isotopic integrity of the studied fossils. Furthermore, in order to explore the habitat preferences, migration and behaviour of *Triceratops*, we conduct histological and stable isotope analyses of accretionary growth trajectories in enamel of multiple teeth to provide constraints on intra- and interannual variability in diet and local hydroclimatic conditions. This new isotopic dataset further allows for direct comparison and integration with other coeval stable isotope datasets, ultimately contributing to a more detailed understanding of Late Cretaceous dinosaur ecosystems of North America. Furthermore, sedimentological analysis of the DTB has been carried out to better constrain its depositional setting and taphonomy.

2. Background

2.1. Geological background

The DTB is a monospecific multi-generational mass death assemblage discovered in western Wyoming, USA on the south-eastern flank of the Powder River Basin (43°36′26.1″N, 104°23′29.3″W; Kaskes et al., 2016). The bonebed is part of the Upper Maastrichtian terrestrial Lance Formation (Bartos et al., 2021) and is dated at ~67 Ma, based on its stratigraphic proximity to the underlying Fox Hills Formation. Five *Triceratops* individuals are identified as *Triceratops horridus* based on the recovered diagnostic cranial elements (Bastiaans et al., 2016) and relatively lower stratigraphic position in the Lance Formation (Longrich and Field, 2012; Scannella et al., 2014).

2.2. Oxygen and carbon stable isotopes in (palaeo-)environmental reconstructions

Biogenic apatite ($\text{Ca}_{10}(\text{PO}_4)_6(\text{OH})_2$) contains small amounts (< 10%) of structurally-bound carbonate (CO_3^{2-}) from which the carbon and oxygen isotope ratio can be analysed. The oxygen and carbon isotope values (expressed in $\delta^{13}\text{C}$ and $\delta^{18}\text{O}$ relative to reference standard) of the body pool from which the bioapatite carbonate is precipitated reflects that of the ingested food and water (Cerling and Harris, 1999).

Most of the ingested oxygen (and $\delta^{18}\text{O}$) in herbivores is incorporated as free drinking (surface) and/or plant water, which are representatives of local precipitation values (Kohn et al., 1996). The $\delta^{18}\text{O}$ value in

precipitation is dependent on geographical and climatic factors including air temperature, latitude, altitude, storage in ice sheets as well as the precipitation amount effect (Dansgaard, 1964; Koch, 1998). Precipitation has a relatively low $\delta^{18}\text{O}$ signature with increasing latitude and altitude due to the preferential loss of ^{18}O over ^{16}O . Evaporation of surface water and evapotranspiration via plant leaf stomata facilitate the removal of the lighter ^{16}O over the heavier ^{18}O , generating a relative enrichment in ^{18}O relative to the initial rainfall (Barbour, 2007). Foraging herbivores hold a unique $\delta^{18}\text{O}$ signal as a function of this ingested plant and drinking water, which is further metabolically modified (e.g., homeothermic vs. poikilothermic) by transpiration and body temperature (Pecquerie et al., 2010; Vander Zanden et al., 2015; Rey et al., 2017) as well as habitat use (Amiot et al., 2006; Amiot et al., 2010). The sum of these factors results in a specific $\delta^{18}\text{O}$ signal recorded in the bioapatite of a (fossil) animal (i.e., bone, dentine, enamel(oid)) and reflects the climatic conditions of that time interval (Kohn and Cerling, 2002; Fricke and Pearson, 2008).

The carbon isotope ratio ($\delta^{13}\text{C}$) stored in vertebrate hard tissues is incorporated from ingested plant material during feeding (Passey et al., 2005). The biochemical pathways of plants involved in the fixation of atmospheric CO_2 during photosynthesis cause a preferential uptake of ^{12}C over ^{13}C . Plants may employ different biochemical pathways to fixate CO_2 during photosynthesis, but temperate C3 plants are most common (Taiz et al., 2015) (C4 plants date back to only 34–24 Ma (Sage, 2004)). Fixation of atmospheric CO_2 by C3 plants result in an offset of on average – 19.5 ‰ (Smith and Epstein, 1971; Kohn and Cerling, 2002; Kohn, 2010) with atmospheric $\delta^{13}\text{C}$ of –6.5 ‰ (pre-industrial) (Graven et al., 2020). Typical C3 modern plant organic matter thus shows an average $\delta^{13}\text{C}$ of -26 ± 2.3 ‰, but covers a wider range of –35 ‰ to –22 ‰ $\delta^{13}\text{C}$ (Kohn, 2010). This atmospheric carbon fixation may thus further vary depending on the environmental conditions including, but not limited to, air temperature, water or nutrient availability and light intensity (Tieszen, 1991). The isotopic offset between the plant diet and tooth enamel for herbivorous mammals shows an average of 14.1 ± 0.5 ‰ (Cerling and Harris, 1999), but this trophic enrichment factor may show a wider range extending beyond 10 ‰ to 15 ‰ based on inter-specific physiological and metabolic differences as well as body size differences (Passey et al., 2005; Tejada-Lara et al., 2018; Rey et al., 2020). On average, this offset between the plant carbon composition and tooth enamel in C3 grazers results in a $\delta^{13}\text{C}$ of ~ –12 ‰ for modern mammals. However, the actual offsets within mammal enamel range from –20 ‰ to –4 ‰ depending on the aforementioned animal and plant physiology as well as environmental and climatic factors (Cerling et al., 1997). Ultimately, the preserved carbon isotopes in (fossil) bioapatite provide insights into the animal’s feeding habits and shed light on their (palaeo)environment.

2.3. Stable isotopes in bioapatite

Preservation of the primary $\delta^{13}\text{C}$ and $\delta^{18}\text{O}$ signal inside the crystal lattice of bioapatitic tissues strongly varies among each tissue type. For example, bones possess relatively high amounts of organic collagen (~30%) and miniscule apatite crystals that provide increased surface areas for in vivo and post-mortem isotopic exchange during recrystallisation and/or incorporation of secondary carbonates (Glimcher, 2006; Schwarcz, 2015, October; Kendall et al., 2018). Additionally, in vivo dynamics of bone growth during the development and remodelling of the vertebrate skeleton (de Buffrénil et al., 2021) leads to averaging of the $\delta^{13}\text{C}$ and $\delta^{18}\text{O}$ over the animal’s lifespan. The crystal lattice of tooth dentine possesses comparably sized small apatite crystals but contains significantly less pore spaces and organic collagen. Conversely, tooth enamel and the equivalent ganoine of lepisosteid scales both consist of larger and stable apatite crystals (< 3% organic collagen), providing relatively less surface area for isotopic exchange, allowing enamel and ganoine to better retain the primary isotope signature during/after diagenesis (Trueman et al., 2003; Fricke et al., 2008). Comparison of

isotope values in different tissue types allows to evaluate the extent of the geochemical alteration of the original isotope signatures. Paired values of enamel and dentine in individual teeth as well as bioapatitic tissues from various sympatric animals occupying distinct habitats may identify diagenetic overprinting across a single locality (Stanton Thomas and Carlson, 2004; Wang et al., 2008; Terrill et al., 2020).

2.4. Sclerochronology

Growth dynamics of various bioapatites follow an accretionary time-related succession (Horner et al., 2000; Tütken et al., 2004; Woodward et al., 2014) such that growth lines are deposited annually in compact bone (Waskow and Sander, 2014; Erickson et al., 2017), whereas dentine and enamel growth lines (lines of von Ebner and Retzius, respectively) are laid down daily (Erickson, 1996; FitzGerald, 1998; Smith, 2006; Tafforeau et al., 2007). Temporal growth trajectories in bone and dental tissues have extensively been studied (Carlson, 1990; Hwang, 2005; O'Meara et al., 2018) and used to reconstruct the growth and estimate the age of (fossil) vertebrates (Erickson, 1996; Waskow and Sander, 2014; Erickson et al., 2017). Despite ceratopsian dinosaurs having poorly developed lines of Retzius (Sander, 1999), it is reasonable to assume that *Triceratops* showed a similar tooth growth pattern as seen in many other vertebrates and a sequence along the length of the enamel surface thus represents a temporal series (Line, 2000).

3. Materials and methods

3.1. Material for palaeoecological analysis

The DTB yielded fossil tooth material of varying degrees of preservation including 63 disarticulated *Triceratops* teeth, seven *Champsosaurus* teeth and eight lepisosteid scales. The *Champsosaurus* teeth were identified as such based on the presence of a clear carina on the anterior and posterior side (Njau and Blumenshine, 2006) and the presence of diagnostic post-cranial *Champsosaurus* material. Selection of teeth for analysis was made based on the preservation: only elements with intact enamel/ganoine surfaces preserved in sufficient detail to allow for an unambiguous identification were selected for isotope sampling. Based on these criteria, a total of fifteen disarticulated *Triceratops* teeth, three aquatic reptile teeth and six lepisosteid scales were used to explore the isotope profile of the DTB ecosystem. In addition, cortical and cancellous bone of two fossil bone fragments were sampled to map the isotope variation in different apatitic tissues. *Champsosaurus* and lepisosteids are representatives of the local fauna that characterized this locality and their isotope signatures inform on the overall palaeoecology of this assemblage.

3.2. Tooth microscopy

In addition, one fully intact *Triceratops* tooth (RGM.1333602) was transversely sectioned to further evaluate the preservation of the studied material. Thin-sectioning was performed following standard procedure by mounting on a glass plate and grinding until the desired thickness for optical microscopy was reached. The thin-section was studied to check for any (taphonomic) damage such as infill of fractures and cavities overprinting the original enamel and dentine part, and photographed using a Nikon Eclipse 50i POL Polarizing Microscope.

3.3. Isotopic sampling of the Darnell *Triceratops* Bonebed

Prior to sampling, the material was cleaned with acetone to remove any possible traces of finger grease, glue residue and other exogenous material. The *Triceratops* teeth were sampled with a diamond-tipped drill bit (1.6 mm diameter) mounted on a Proxxon Micromot hand-held drill. All fourteen *Triceratops* teeth were sampled for their enamel and dentine content. A total of seven teeth preserving a complete crown

were used for serial sampling. All serial-sampled teeth belong to adult individuals based on size. However, the sample selection is represented by unworn and worn teeth, providing a transect in tooth size and difference in sample area for each individual tooth (see Supplements Fig. S3 for overview). Serial samples were taken along the growth axis of each, resulting in three samples for the smallest tooth and eight samples for the largest tooth. The other remaining seven teeth were too small or too fragmented for serial sampling and are represented only by one single sample. These samples were acquired only from areas with intact enamel. The thin-sectioned tooth provided guidance on the ideal drilling depth based on the enamel thickness and state of preservation (Fig. 3), and the enamel was clearly delineated from the dentine based on colour and density. Single samples of the *Champsosaurus* teeth and the lepisosteid scales were acquired using the same method, but their small sizes did not permit serial sampling. Fossil bone samples were also retrieved in singles and are represented by cortical and medullary bone. Powdered samples were collected on weighing paper and transferred into 2.5 ml Eppendorf centrifuge tubes. Prior to sampling, the drill bit was blasted with nitrogen gas to remove possible adhering sample powder. Each collected powder sample was ~0.7 mg.

A selection of samples was leached according to the protocol described in Koch et al. (1997). It has been shown that different pretreatment strategies may cause a shift in isotopic data due to removal of exogenous (i.e., diagenetic) material from (dental) bioapatite such as enamel and dentine (Lee-Thorp and Van der Merwe, 1987; Lee-Thorp and van der Merwe, 1991; Krueger, 1991; Wang and Cerling, 1994; Koch et al., 1997). Bioapatite powder samples of three *Triceratops* teeth, a *Triceratops* bone fragment, two *Champsosaurus* teeth and three lepisosteid scales retrieved during sampling were split to explore the impact of different pretreatment protocols (Fig. 2). Selected samples were either first soaked overnight in sodium hypochlorite (NaOCl) for oxidation or left untreated. Both groups were then rinsed three times with MilliQ water, and soaked overnight in either 0.1 M acetic acid or 1 M acetic acid buffered with calcium acetate creating additional aliquots (Koch et al., 1997). Finally, all groups were rinsed three times again with MilliQ water and dried at 60°C. Proportions were kept constant between apatite sample powder and fluids during leaching and oxidation (0.04 ml/mg) to avoid imbalanced reactions (Koch et al., 1997). The samples were left for 24 h to react overnight.

After drying, isotope samples were transferred to exetainer vials with pierceable endcaps and flushed with pure helium and subsequently digested through a Thermo Scientific Gasbench II in 100% water-free phosphoric acid. The formed CO₂ from the structural carbonate part was then analysed for their carbon and oxygen isotope signature by a Finnigan MAT253 Isotope Ratio Mass Spectrometer (IRMS) housed at the Earth Sciences Stable Isotope Laboratory at the Faculty of Science at the Vrije Universiteit (VU) in Amsterdam, the Netherlands. Different amounts of the VU Internal Carbonate Standard (VICS) have been analysed in each run for correction of the so-called sample amount effect. In each run, the IAEA-603 standard (2.49 ± 0.07 ‰ for $\delta^{13}\text{C}$ and -2.40 ± 0.07 ‰ for $\delta^{18}\text{O}$ (1σ , $n = 17$)) was routinely analysed as an independent control standard with internationally accepted $\delta^{13}\text{C}$ and $\delta^{18}\text{O}$ values of 2.46 ± 0.01 ‰ and -2.37 ± 0.04 ‰, respectively (Assonov et al., 2020). The inter-laboratorial apatite standard Ag-lox is also analysed in each run providing mean $\delta^{13}\text{C}$ and $\delta^{18}\text{O}$ values of -11.62 ± 0.07 ‰ and -0.94 ± 0.22 ‰ ($n = 11$), respectively, in agreement with the long-term means of -11.62 ‰ and -0.99 ‰ at 45 °C ($n = 95$, VU). In contrast to the $\delta^{13}\text{C}$ values, ~0.5 ‰ lower $\delta^{18}\text{O}$ values were obtained at 70 °C (Vanhof et al., 2020), which can be attributed to the temperature-dependent fractionation factor between the generated CO₂ and structurally-bound carbonate in apatite during acid digestions that may slightly differ from that of the standards that were used for the linearity corrections (LSVEC and BCT for $\delta^{13}\text{C}$, and NBS-18 and BCT for $\delta^{18}\text{O}$ (Kim et al., 2015)). Its long-term precision of the apatite standard measurements was determined <0.1 ‰ for $\delta^{13}\text{C}$ and <0.2 ‰ for $\delta^{18}\text{O}$. The isotopic compositions were initially expressed in standard notation

relative to the international standard Vienna Pee Dee Belemnite (VPDB). Hereafter, the $\delta^{18}\text{O}$ values were converted to Vienna Standard Mean Ocean Water (VSMOW) according to Coplen (1988) (p. 295, formula [11]) allowing for comparison with previous studies on Late Cretaceous $\delta^{18}\text{O}$ datasets. In order to estimate the $\delta^{18}\text{O}$ of the local (drinking) water ($\delta^{18}\text{O}_w$) from the *Triceratops* enamel structural carbonate ($\delta^{18}\text{O}_{sc}$), we applied the formula established for large, water-dependent herbivores by Hoppe (2006) (see section 6.2 for details):

$$\text{Mean } \delta^{18}\text{O}_{sc} = 30.32 (\pm 1.23) + (0.73 (\pm 0.10) \cdot \text{Mean } \delta^{18}\text{O}_w) \quad (1)$$

3.4. Diagenetic screening

To evaluate the chemical preservation of the *Triceratops* material and extent of specific leaching effects, remaining subsets of untreated and leached powder samples from the DTB were analysed for their calcium/phosphorous (Ca/P) ratios using scanning electron microscopy (SEM) with Energy Dispersive X-Ray Spectroscopy (EDS) at the VU (see Supplementary Raw Data for sample details). Approximately 0.7 mg of sample powder of each bioapatite tissue type (enamel, dentine and bone) covering three treatment strategies (untreated, 0.1 M acetic acid and 1 M calcium acetate buffer) were applied on a carbon sticker and analysed in vacuum by a JEOL JCM-600 SEM. Additionally, *Triceratops* tooth fragments and the open thick section (Fig. 3) were analysed for their elemental composition. Modern human tooth fragments were analysed to provide a modern baseline for bioapatite. Each *Triceratops* sample was measured six times and the average was used for data interpretation. The Ca/P ratio is known to shift during diagenesis of the original bioapatite (Herwartz et al., 2011; Tütken et al., 2011; Herwartz et al., 2013; Trueman, 2013), and comparing the Ca/P of fossil bioapatite to modern bioapatite therefore provides information on the degree of diagenetic alterations.

In addition, Fourier-transform infrared spectroscopy (FTIR) was performed using the KBr-pellet method to better constrain mineralogical changes due to fossilisation and leaching strategies applied here. Like for Ca/P ratios, FTIR analyses were applied to all three bioapatite tissues and pretreatment strategies using material from the DTB. Approximately 7 mg of sample powder was mixed and ground with oven-dried KBr powder in a 1:100 ratio (1%) using an agate mortar and pestle. The resulted powder mix was then pressed into a ~3 mm pellet at 10 ton pressure using a hydraulic press. Pellets were transferred into a holder and measured in a Nicolet 6700 FTIR analyser housed at Utrecht University, Faculty of Geosciences, the Netherlands. The acquired spectra were created and analysed using OMNIC software. Each sample mixture yielded three pellets that were measured and their average spectrum was used as end results. Each new sample was standardized using its own 100% KBr pellet background. Spectra were used to calculate the carbonate:phosphate (C/P) ratios and the infrared splitting factors (IR-SF; i.e., crystallinity index). C/P ratios were quantified by dividing the carbonate absorbance peak at 1415 cm^{-1} and the phosphate absorbance peak at 1035 cm^{-1} (Wright and Schwarcz, 1996). The IR-SF values were obtained by adding the two phosphate absorbance peaks at 605 cm^{-1} and 565 cm^{-1} and dividing by the lowest value between those peaks at 590 cm^{-1} (Weiner and Bar-Yosef, 1990).

3.5. Sedimentological analysis

Geological fieldwork and excavations at the DTB by Naturalis Biodiversity Center (2015–2019) included detailed lithostratigraphic analysis of the bone-bearing layer (Fig. 1). Sedimentary successions bounding the DTB were sampled at 10 cm resolution to analyse lithogenic grain-size properties, organic and carbonate contents of the sediments ($n = 7$) with the aim to better understand the palaeoenvironmental and depositional conditions.

Grain size analyses were conducted at the Sediment Laboratory of the Vrije Universiteit (VU) Amsterdam using a Sympatec HELOS KR

laser-diffraction particle size analyser. Prior to the grain size analysis, the bulk sediment samples were pretreated to isolate the lithogenic fraction following the procedure by Konert and Vandenberghe (1997). Organic matter and carbonate material was removed by treating the samples with 5–10 ml of 30% H_2O_2 and 5–10 ml of 10% HCl, respectively.

Total organic and carbonate contents were measured through thermogravimetric analysis using a thermogravimetric analyser (LECO TGA 701) instrument at the Sediment Laboratory of the VU. Sediment samples were carefully grinded with mortar and pestle into a homogeneous powder. Approximately 1–2 g per sample powder was analysed by sequential loss-on-ignition using step-wise heating from 25 to 1000°C until the sample weights stabilized. The associated weight loss per temperature step is used to determine the total organic content (i.e., at max 550°C ; LOI550) and calcium carbonate content (i.e., at max 1000°C ; LOI1000) within the bulk sediment. All of the used data can be found in the Supplementary Raw Data file.

4. Results

4.1. Sedimentological setting

The ~1.1 m thick stratigraphic section exposed at the DTB comprises an alternation of mudstone, fine-grained sandstone, and siltstone with an average organic and carbonate content of 3.2 wt% and 2.4 wt%, respectively. The section can be divided in three distinct sedimentary units (Fig. 1B,C). The basal unit of the DTB (~70 cm) yields the remains of at least five *Triceratops* individuals and is dominated by a purple-grey mudstone with a relatively high organic content (up to 4.6 wt%) due to abundant plant remains. The second unit of the DTB consists of a thin (10–20 cm thick) layer of a yellowish, very fine sandstone. The base of this unit is marked by an erosional contact with convolute lamination and siltstone flame structures (Fig. 1B). The third stratum (~20 cm) is dominated by a brown sandy siltstone unit with sandy lenses and plant remains. The CaCO_3 content is on average low (2.4 wt%) with maximum values of 3.6 wt% and 4.2 wt% in the sandstone layer.

4.2. Tooth microstructure

Visual inspection of the tooth thin-section indicates that the dental material is relatively well-preserved, as all of the histological features seem to remain unchanged (Fig. 3). The enamel is clearly visible as a transparent band varying from 0.1 to 0.3 mm on the buccal side and a similar, but thinner band on the lingual side. The enamel thickness is in line with previously established enamel thickness for ceratopsids and *Triceratops* in particular (Sander, 1999; Hwang, 2005) confirming that our sampling approach aiming at the enamel separate from the dentine is feasible. The dentine displays incremental lines of Von Ebner (von Ebner, 1902), but their visibility and quantity varied throughout the section. At the highest, a total of 91 incremental growth lines are counted (Fig. 3), indicating that the sclerochronological record preserved in the tooth covers some three months (Erickson, 1996; Fitzgerald, 1998; Smith, 2006; Tafforeau et al., 2007). Some areas display small localized fractures, but the overall preservation of dental features suggests that most of the apatite tissues did not undergo major post-mortem alteration.

4.3. Effects of pretreatment

The pretreatment procedures showed significant effects among the different apatitic tissue samples, but do not display unidirectional offsets between treated and untreated samples for the different leaching procedures (Fig. 4). Pretreatment of *Triceratops* enamel resulted in significantly higher $\delta^{18}\text{O}$ values than untreated enamel ($p = 0.00$), while $\delta^{13}\text{C}$ seemed unaffected ($p = 0.17$). For *Triceratops* dentine, the effects of the pretreatment result in both higher $\delta^{18}\text{O}$ and $\delta^{13}\text{C}$ values ($p = 0.00$ for

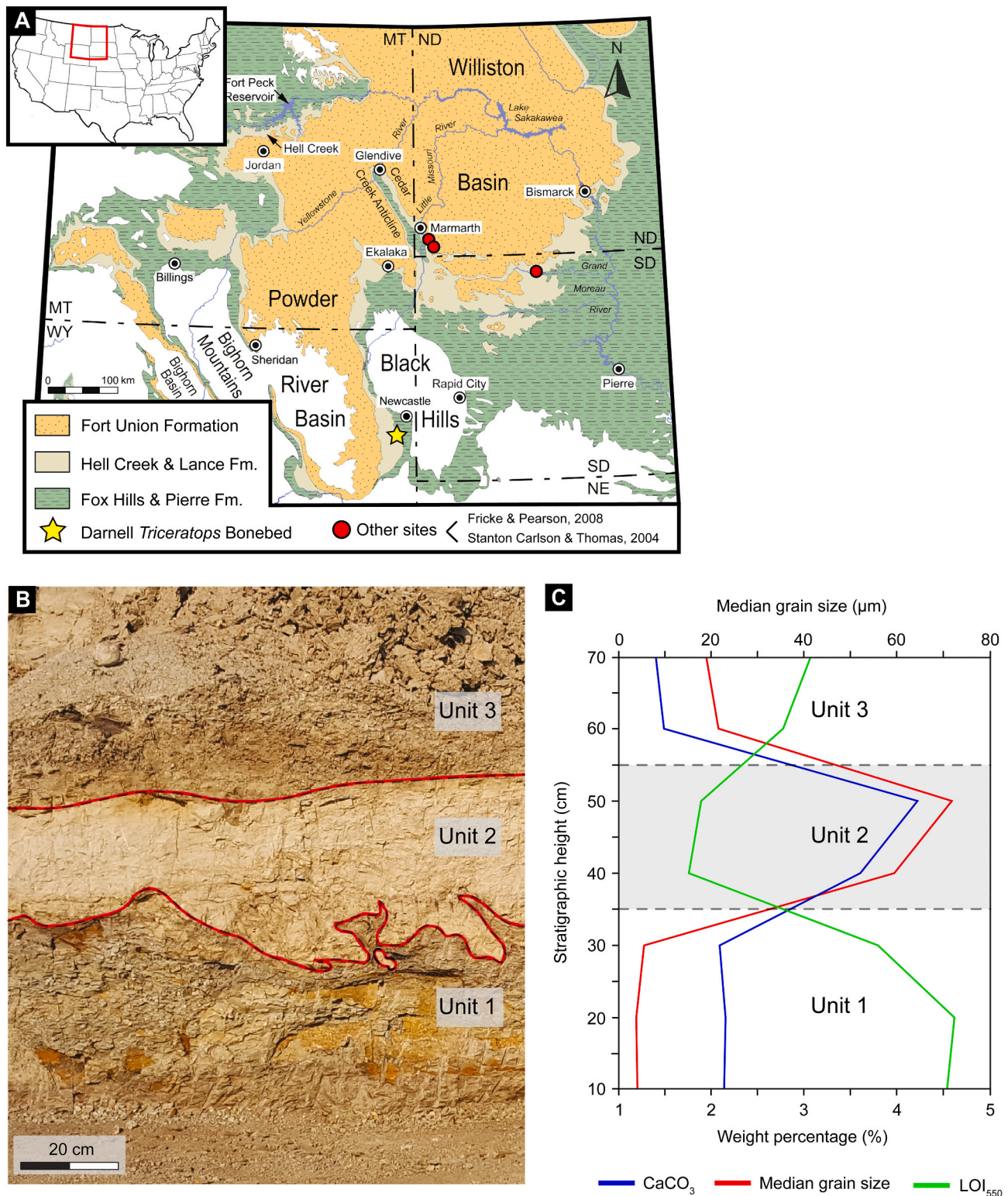


Fig. 1. Geography, sedimentology and lithostratigraphy of the sedimentary succession bordering the DTB. **A.** Geological map of the Williston Basin and Powder River Basin in Wyoming, Montana, South Dakota and North Dakota, displaying the distribution of Upper Cretaceous to Paleocene rock formations (modified from Johnson et al., 2002; Fastovsky and Bercovici, 2016). The Darnell *Triceratops* Bonebed, located in the Lance Formation ~30 km south of Newcastle, is highlighted with a yellow star. Also depicted here are vertebrate sites from the Hell Creek Formation of North Dakota (Fricke and Pearson, 2008) and South Dakota (Stanton Thomas and Carlson, 2004), which datasets are used in this isotopic study as a comparison in Fig. 12. **B.** Field photo depicting the sedimentary succession representing the bonebed layer. Photo taken in eastern direction. **C.** Total organic content (LOI_{550} , in wt%), median lithogenic grain size (in μm) and carbonate content (CaCO_3 , in wt %) of the sedimentary succession. Data (C) is plotted against stratigraphic height, and are correlated with the stratigraphy in the field photo (B). Note the marked increase in grain size in the crevasse splay deposit (Unit 2), which is bounded by the red line. (For interpretation of the references to colour in this figure legend, the reader is referred to the web version of this article.)

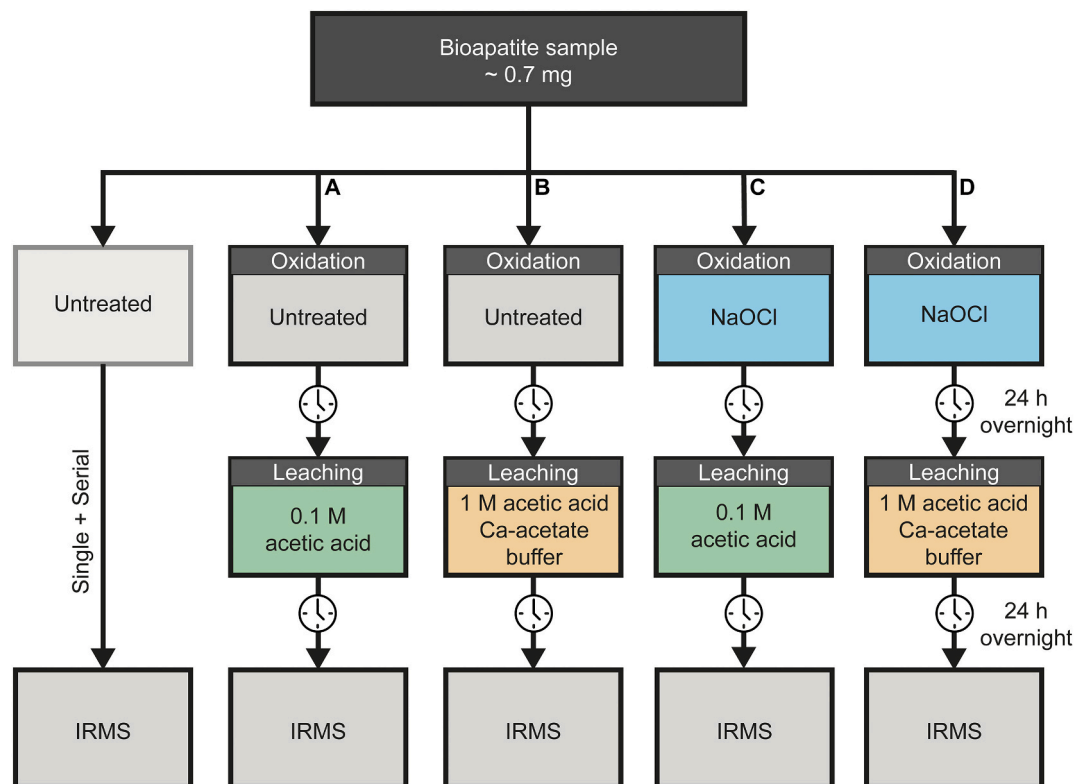


Fig. 2. Overview of the four different pretreatment protocols applied to the bioapatite samples. Treatments were applied as a combination of different oxidation and leaching steps.

both). *Triceratops* bone did not show a shift in $\delta^{18}\text{O}$ after leaching ($p = 0.92$), but had significantly increased $\delta^{13}\text{C}$ values ($p = 0.04$). Bone is the least affected by pretreatments while dentine shows the strongest shifts between strategies. Strikingly, dentine δ -values became more positive after treatment, diverting from enamel δ -values. This contradicts the assumption that removal of labile material would produce a signal more resembling the enamel δ -values, which are assumed less prone to diagenesis. Treatment of *Champsosaurus* enamel shifted the $\delta^{18}\text{O}$ values ($p = 0.05$), but the $\delta^{13}\text{C}$ values did not show a significant change ($p = 0.06$). *Champsosaurus* dentine $\delta^{18}\text{O}$ and $\delta^{13}\text{C}$ values on the other hand both increased after the leaching treatment ($p = 0.00$ and $p = 0.04$, respectively). Similarly, lepisosteid ganoine $\delta^{18}\text{O}$ and $\delta^{13}\text{C}$ values were significantly higher for the treated samples ($p = 0.01$ and $p = 0.00$, respectively). The data on the sample treatment do not give unanimous results regarding the possible effects of diagenesis on the different tissues and taxa.

Similar trends are observed in the Ca/P ratios of dinosaur bioapatite, which overlap with known modern bioapatite values of ~ 2.3 (Balter, 2001; Hassler et al., 2018). Moreover, average measured Ca/P ratios of untreated and leached tooth bioapatite overlap with each other and with modern human enamel, and fail to detect any significant differences in the dataset (Fig. 5 & Table 1; Kruskal-Wallis test, $p = 0.051$). Only *Triceratops* bone showed larger spread in their Ca/P ratios, but dentine and enamel closely overlap for each treatment strategy. Additionally, the FTIR analyses provided ambiguous results regarding the effects of the sample pretreatments (Table 1). Modern bone values are commonly measured at C/P ratio of 0.23–0.34 (Wright and Schwarcz, 1996; Nielsen-Marsh and Hedges, 2000; Garvie-Lok et al., 2004; Beasley et al., 2014) and an IR-SF of 2.50–3.25 (Berna et al., 2004; Thompson et al., 2009; Beasley et al., 2014). While treated *Triceratops* enamel bioapatite show C/P and IR-SF values more akin to modern bone values, both enamel leached by 0.1 M acetic acid and leached by 1 M calcium buffer fail to fall within modern ranges (Table 1). In fact, leaching with 1 M calcium buffer increased the C/P and IR-SF values far beyond modern

ranges. Interestingly, dentine bioapatite shows steady IR-SF values throughout the three treatment strategies. C/P values vary slightly more, but all treatment strategies overshoot modern values. Contradicting to accepted theory on diagenesis, untreated bone seems best preserved, with values most akin to modern values for both C/P ratios and IR-SF data. Both leaching strategies result in greatly increased C/P ratios and IR-SF values, but the change is largest for treatment with 0.1 M acetic acid. Overall, the pretreatment strategies discussed here show no consistent pattern in shifts in C/P and IR-SF data across different bioapatite tissues, and the FTIR spectra indicate only slight diagenetic alteration of *Triceratops* enamel (Fig. 6).

While leaching pretreatments could provide more accurate isotope data, it has been found that oxidation and leaching can also have adverse effects (Koch et al., 1997; Lee-Thorp, 2002; Pellegrini et al., 2011; Snoeck and Pellegrini, 2015; Pellegrini and Snoeck, 2016). The samples were left for 24 h to react, which might have induced adverse effects, in particular NaOCl which could promote the (re-)precipitation of secondary carbonate that is equilibrated with atmospheric CO_2 (Zazzo et al., 2004; Snoeck and Pellegrini, 2015; Pellegrini and Snoeck, 2016). On the other hand, it is expected that these secondary carbonates are dissolved during the subsequent leaching step. The non-systematic isotopic responses of the various apatite tissues indicate that not simply labile carbonates and eventual organic matter were stripped, but that complex reactions may have taken place during different pretreatment procedures, doing potentially more harm than good. Furthermore, the sediment matrix of the bonebed is virtually free of CaCO_3 (Fig. 1), considerably reducing the chance of precipitation of secondary carbonates and isotopic overprint. Considering the overall ambiguous result and nonconformity across the pretreatment data, the Ca/P calculations and the FTIR data, we chose to focus on the untreated data only for the remainder of this paper to represent the bonebed (c.f., Janssen et al., 2016) (see section 6.1 for more details).

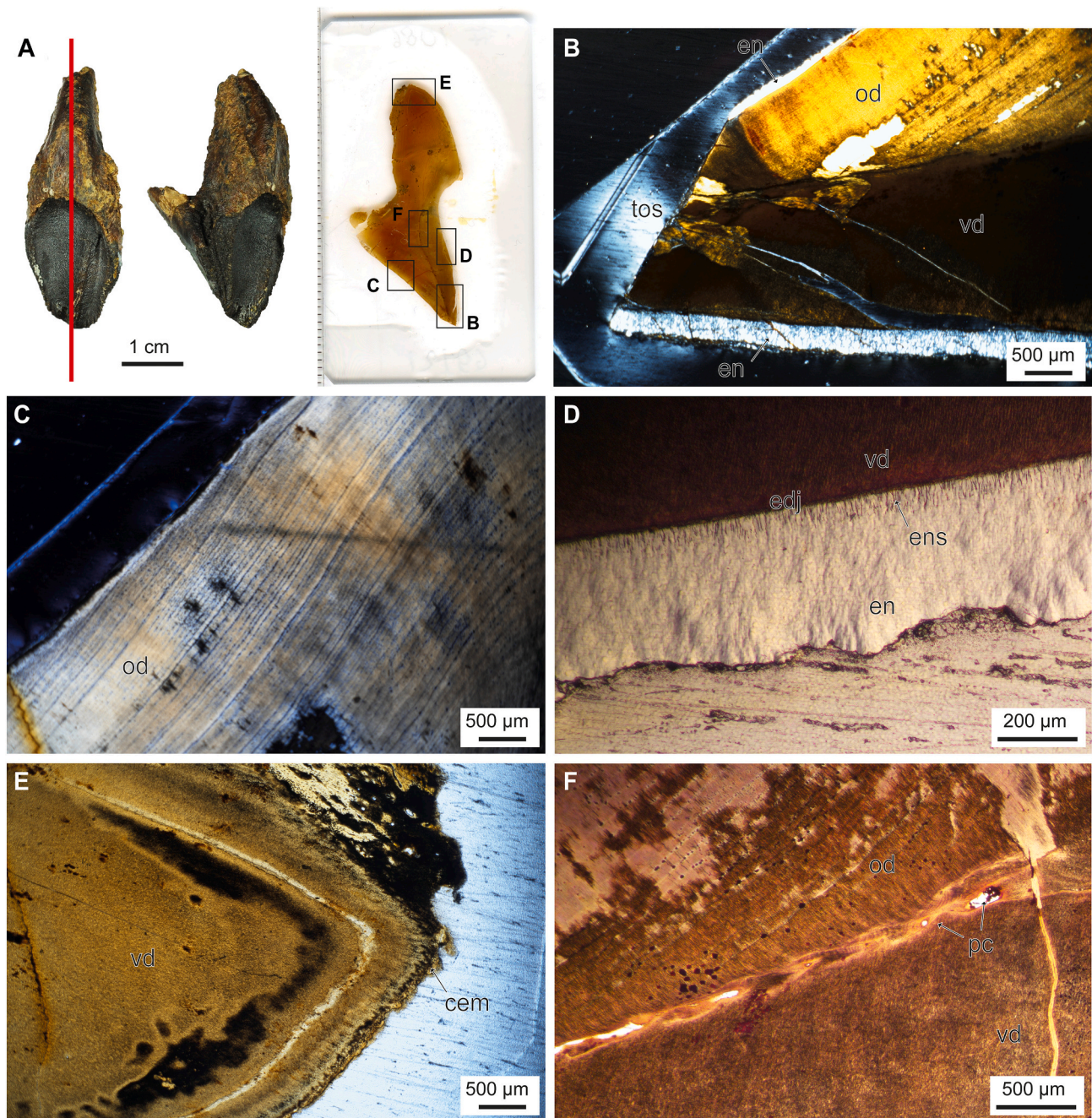


Fig. 3. Histology of an adult *Triceratops* tooth. A. Intact *Triceratops* tooth (RGM. 1,333,602) showing plane of section (red line) and thin-section. B. Tooth apex under cross-polarized light. C. Orthodentine containing Von Ebner lines. D. Closeup of enamel showing enamel spindles protruding from the enamel-dentine junction. E. Tooth root apex with cementum. F. Dentine matrix with pulp cavity. cem, cementum; edj, enamel-dentine junction; en, enamel; ens, enamel spindles; od, orthodentine; pc, pulp cavity; vd, vasodentine. (For interpretation of the references to colour in this figure legend, the reader is referred to the web version of this article.)

4.4. Isotope systematics among different bioapatite tissues

Fig. 7 displays the isotope signatures of the different bioapatitic tissues among different taxa on all isotopic datasets. Detailed statistical analyses and data exploration are provided in the Supplements (Table S1-S4, Fig. S1 & S2). A non-parametric Kruskal-Wallis test with Bonferroni correction did not return a significant difference ($p = 0.15$) between the lower mean $\delta^{18}\text{O}$ values of *Triceratops* enamel (19.4 ‰) and the higher *Triceratops* dentine (20.0 ‰, $p = 0.23$). For carbon, the mean *Triceratops* dentine $\delta^{13}\text{C}$ values (0.14 ‰) were significantly higher ($p = 0.00$) than those of *Triceratops* enamel (−5.4 ‰). *Triceratops* bone $\delta^{13}\text{C}$ values (−3.4 ‰) are significantly lower than those of dentine ($p = 0.00$)

and are markedly higher than mean enamel values ($p = 0.02$). However, the mean *Triceratops* bone $\delta^{18}\text{O}$ value (19.8 ‰) do not seem to differ from enamel and dentine $\delta^{18}\text{O}$ ($p = 0.26$ and $p = 1$, respectively). Isotopic offsets between bioapatitic tissues are more pronounced in the $\delta^{13}\text{C}$ values than $\delta^{18}\text{O}$ values. This is further emphasized by the applied paired Kruskal-Wallis test, where mean $\delta^{18}\text{O}$ values between apatite groups fall outside the range of significance ($p = 0.15$) while $\delta^{13}\text{C}$ values still show strong significant differences among all apatitic tissue groups ($p = 0.00$).

Plotting the enamel and dentine isotopic values of the same tooth reveals a similar pattern (Fig. 10). For $\delta^{18}\text{O}$, differences in enamel and dentine within individual teeth ($\Delta\delta^{18}\text{O}_{\text{e-d}}$) were significantly lower than

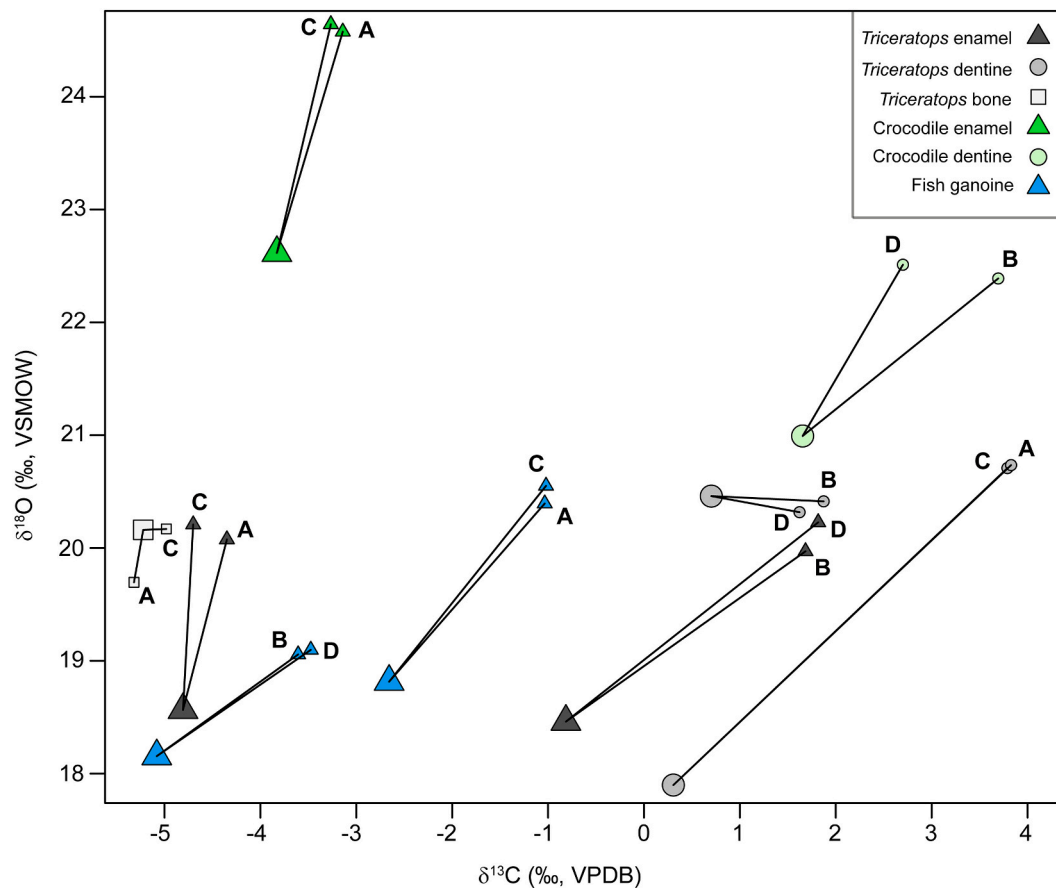


Fig. 4. Crossplot showing the effects of the different pretreatment groups across different bioapatite tissues and taxa. The large symbols represent the $\delta^{18}\text{O}$ and $\delta^{13}\text{C}$ of the untreated bulk data. The connecting smaller symbols associated with the letter 'A', 'B', 'C', or 'D' represent $\delta^{18}\text{O}$ and $\delta^{13}\text{C}$ values of the same samples but treated by four different combinations of oxidation and leaching steps: A) leached with 0.1 M acetic acid, B) leached with 1 M calcium buffer, C) NaOCl oxidation and leached with 0.1 M acetic acid and D) NaOCl oxidation and leached with 1 M calcium buffer.

observed for $\delta^{13}\text{C}$ ($\Delta\delta^{13}\text{C}_{\text{e-d}}$). There is no systematic pattern in the degree of isotopic offset among all the sampled teeth for $\delta^{13}\text{C}$ or $\delta^{18}\text{O}$ values. However, a general trend is visible within individual teeth showing similar relative changes in $\Delta\delta^{18}\text{O}_{\text{e-d}}$ and $\Delta\delta^{13}\text{C}_{\text{e-d}}$. In other words, teeth with relatively lower $\Delta\delta^{18}\text{O}_{\text{e-d}}$ also show lower $\Delta\delta^{13}\text{C}_{\text{e-d}}$. Nevertheless, the preserved isotope systematics are in line with the assumed susceptibility to chemical alteration of fossil bioapatite, where lower δ -values from enamel bioapatite resemble the original signal incorporated into the structurally-bound carbonate during metabolic fractionation. In contrast to enamel, dentine and bone bioapatite values become more positive and average out post-mortem, resulting in an isotope signature more akin to the depositional environment (Tütken et al., 2011). This is further emphasized by the larger spread in enamel data ($\delta^{13}\text{C}$: 10.8 ‰ and $\delta^{18}\text{O}$: 6.5 ‰, $n = 60$) and the more restricted dentine data ($\delta^{13}\text{C}$: 7.5 ‰ and $\delta^{18}\text{O}$: 3.1 ‰, $n = 21$) (Figs. 7, 8 and 9). On the other hand, *Champsosaurus* enamel did not significantly differ from *Champsosaurus* dentine for both $\delta^{13}\text{C}$ ($p = 0.11$) and $\delta^{18}\text{O}$ ($p = 1$). This could most likely be attributed to low sample sizes ($n = 3$ and $n = 4$), and we do obtain δ -values that overlap those of *Triceratops* (Le Boedec, 2016). However, rarefying our *Triceratops* enamel $\delta^{13}\text{C}$ and $\delta^{18}\text{O}$ data (see Supplements Fig. S2; recalculating variances based on 1000 random samples of $n = 5$) reveals a markedly lower variance than the original dataset, suggesting unequal variance among taxa, and thus further supports the use of non-parametric Kruskal-Wallis tests.

4.5. Oxygen isotopes

Overall, across all sampled material, *Triceratops* enamel $\delta^{18}\text{O}$ values

(mean 19.4 ‰) show a total range of 6.5 ‰. Dentine $\delta^{18}\text{O}$ values of *Triceratops* (mean 20 ‰) have a slightly smaller range of 3.1 ‰ (Fig. 8). The three available values for *Champsosaurus* enamel $\delta^{18}\text{O}$ (mean 20.5 ‰) show a wider spread of 4.0 ‰, but largely overlap the $\delta^{18}\text{O}$ of *Triceratops* enamel. *Champsosaurus* dentine (mean 20.1 ‰) shows a smaller range of 2.8 ‰. The ganoine of lepisosteid scales (mean 18.5 ‰) span a total range of 4.1 ‰ in $\delta^{18}\text{O}$ values, but also are within range of both *Triceratops* and *Champsosaurus* enamel $\delta^{18}\text{O}$. Non-parametric Kruskal-Wallis test with Bonferroni correction on the enamel/ganoine $\delta^{18}\text{O}$ across the three taxa did not return any significant differences ($p = 0.19$) (Table S4).

The incrementally sampled teeth show extensive overlap in their $\delta^{18}\text{O}$ signatures (Fig. 11), except for one sample that yields a markedly lower $\delta^{18}\text{O}$ value of 15.3 ‰ (RGM.1333595). Variability of $\delta^{18}\text{O}$ within the individual teeth for *Triceratops* enamel ranges from 0.4 ‰ to 4.8 ‰, with the majority having intra-tooth variability lower than 1 ‰. On average, intra-tooth $\delta^{18}\text{O}$ variability for *Triceratops* enamel is 0.8 ‰. The inter-tooth variability of $\delta^{18}\text{O}$ enamel of all serial-sampled *Triceratops* teeth is 5.9 ‰ (15.3 ‰ to 21.2 ‰). This range is on average higher than is observed for sampled *Champsosaurus* enamel (4.0 ‰) and lepisosteids ganoine (4.1 ‰).

4.6. Carbon isotopes

The complete isotope analysis returned a total range of 10.8 ‰ for *Triceratops* enamel $\delta^{13}\text{C}$ (mean -5.4 ‰) and a smaller range of 7.5 ‰ for dentine $\delta^{13}\text{C}$ (mean 0.14 ‰) (Fig. 9). *Champsosaurus* enamel $\delta^{13}\text{C}$ shows a spread of 2.0 ‰ with a mean value of -4.5 ‰. *Champsosaurus* dentine

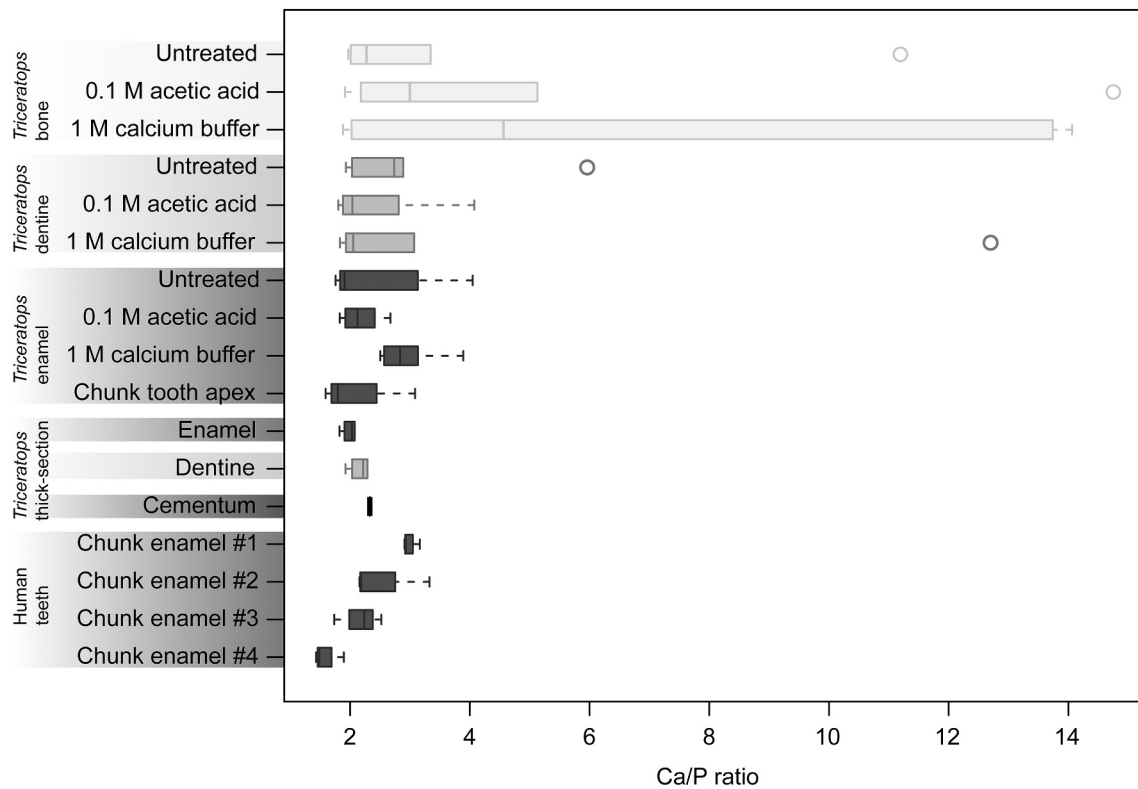


Fig. 5. Boxplots showing the spread in Ca/P ratios across different bioapatite tissues and different pretreatment strategies. Across all sampled material, there is no significant difference in Ca/P ratio between fossil and modern specimens. *Triceratops* bone shows greater spread, most probably because bone is more sensitive to diagenetic effects. See Supplementary Raw Data file for all individual Ca/P measurements.

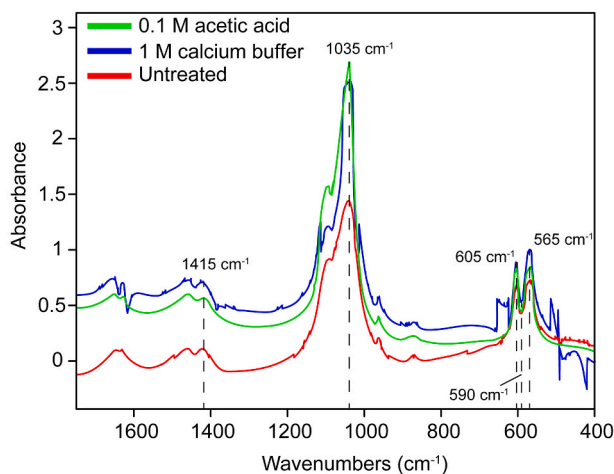


Fig. 6. FTIR spectrum showing *Triceratops* enamel across three different treatment strategies. The indicated peaks are used to calculate C/P ratios (1415/1035) and IR-SF values ((605 + 565)/590).

$\delta^{13}\text{C}$ (mean 0.2 ‰) showed a greater range of 3.1 ‰. Lepisosteid ganoine $\delta^{13}\text{C}$ (mean -3.0 ‰) values spanned a total range of 4.8 ‰. The $\delta^{13}\text{C}$ in the enamel/ganoine of the three taxa are overlapping, but a Kruskal-Wallis test returned a significant difference ($p = 0.01$). Subsequent post-hoc paired Mann-Whitney U tests with Bonferroni correction indicated that only *Triceratops* enamel was significantly different from the lepisosteid ganoine (Table S4).

The incrementally sampled teeth show an overlapping range of enamel $\delta^{13}\text{C}$ values and show slightly stronger fluctuations compared to $\delta^{18}\text{O}$ increments (Fig. 11). The same sample that yielded an unusually

low $\delta^{18}\text{O}$ value also produced a similarly low $\delta^{13}\text{C}$ value (RGM.1333595). Intra-tooth variability among all teeth ranges from 0.6 ‰ to 4.6 ‰ with mean intra-tooth variability calculated at 2.5 ‰. Inter-tooth $\delta^{13}\text{C}$ variability calculated among all the serial sampled *Triceratops* enamel is 8.1 ‰. The same pattern emerges here as with $\delta^{18}\text{O}$ values, where *Triceratops* inter-tooth enamel $\delta^{13}\text{C}$ variability is higher than in *Champsosaurus* and lepisosteids (2.0 ‰ and 4.8 ‰, respectively), although we acknowledge the small dataset for the latter two species.

5. Discussion

5.1. Depositional setting

The organic rich, carbonate poor, fine-grained siliciclastic sediment that embeds the fossil material matches a depositional environment representing a floodplain setting typical for the Late Cretaceous fluvial systems bordering the Western Interior Seaway (Crystal et al., 2019). The organic rich fine-grained basal unit can be interpreted as a residual channel infill deposited in a low energy terrestrial environment. The overlying sandy unit displays typical sedimentary features related to a crevasse splay event (c.f. Burns et al., 2017). The DTB fossil material is well-preserved with limited morphological distortion, retention of original bone surfaces, and only minor weathering and erosion damage. Absence of evidence of scavenging suggests that exposure of the animal carcasses was limited, and that initial burial occurred relatively fast, which is corroborated by the grain size data (Fig. 1C).

5.2. Extent of diagenesis

While there is no single test capable of providing conclusive evidence against (significant) diagenetic alteration, a combination of insights can help to understand the post-mortem alteration of fossil bioapatite for

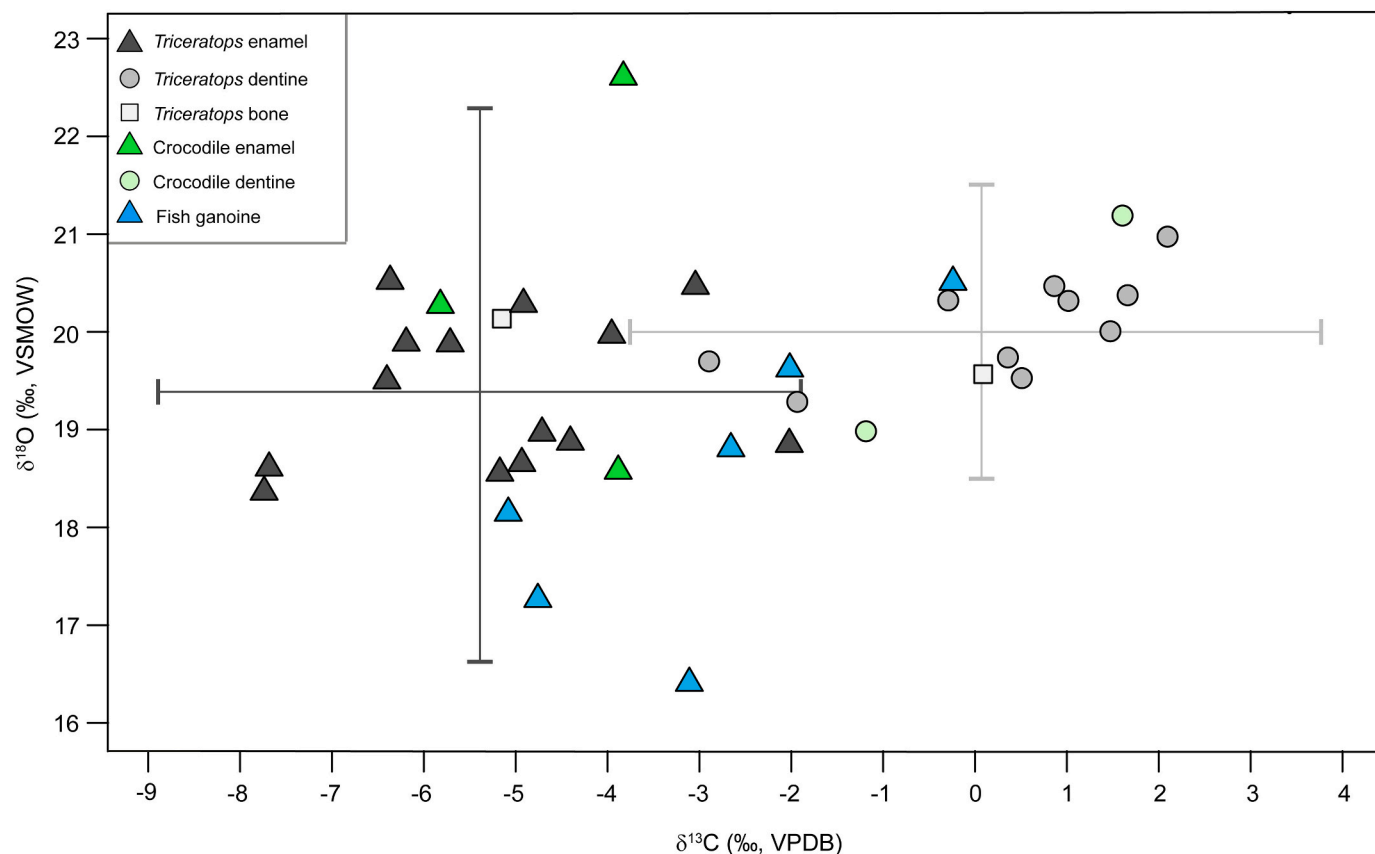


Fig. 7. Crossplot diagram showing the total overview (single and incrementals) of $\delta^{18}\text{O}$ and $\delta^{13}\text{C}$ isotope values across different taxa of the Darnell *Triceratops* Bonebed. Each point represents the average value of a single tooth/scale. Note the more positive values and tighter spread of the dentine values compared to enamel and ganoine. Bone values plot in-between enamel and dentine values. The two crosses represent the spread ($\pm 2\sigma$) for enamel and dentine.

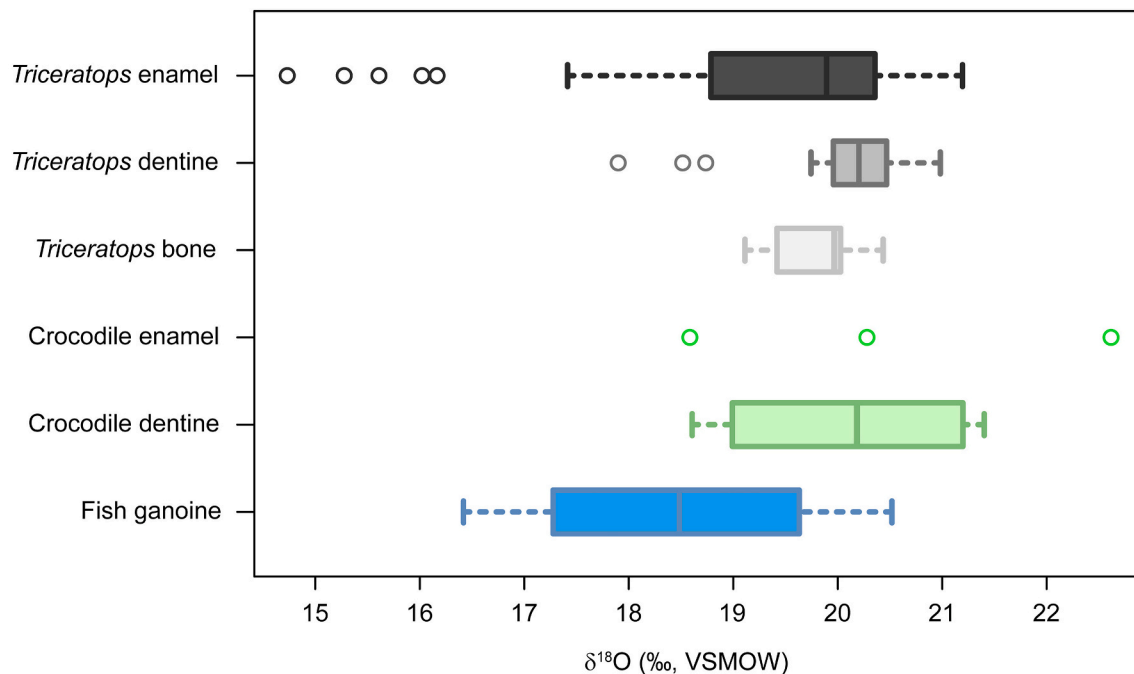


Fig. 8. Boxplots showing the range and spread in $\delta^{18}\text{O}$ of bioapatite tissues from *Triceratops*, *Champsosaurus* and lepisosteids. *Champsosaurus* enamel is represented by three samples only.

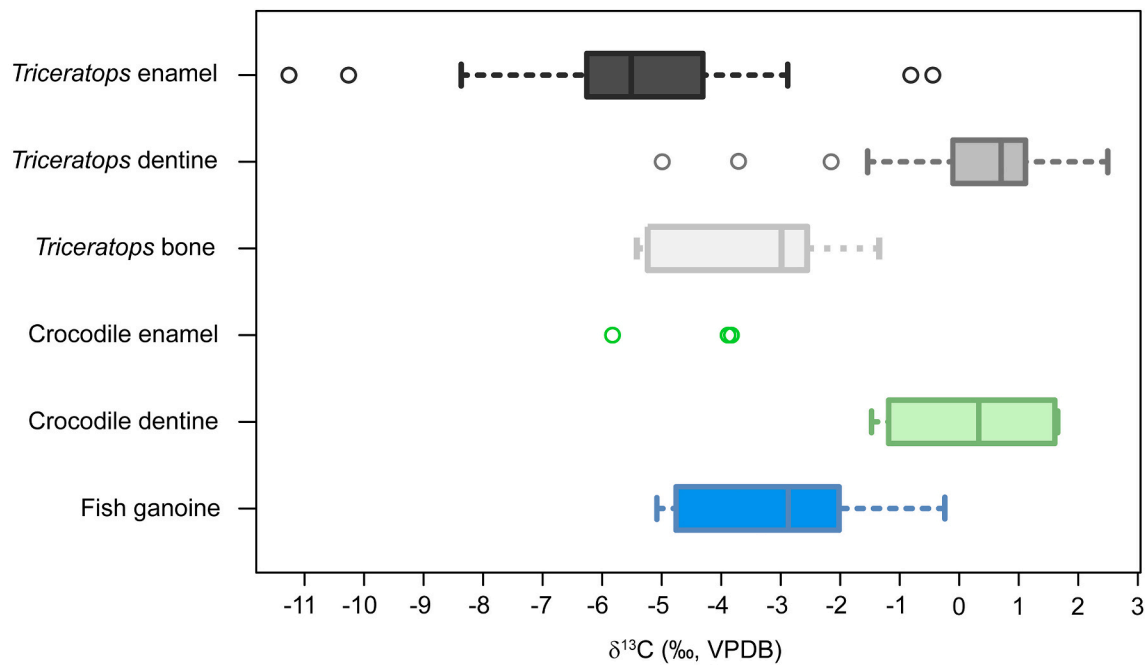


Fig. 9. Boxplots showing the range and spread in $\delta^{13}\text{C}$ of bioapatite tissues from *Triceratops*, *Champsosaurus* and lepisosteids. *Champsosaurus* enamel is represented by three samples.

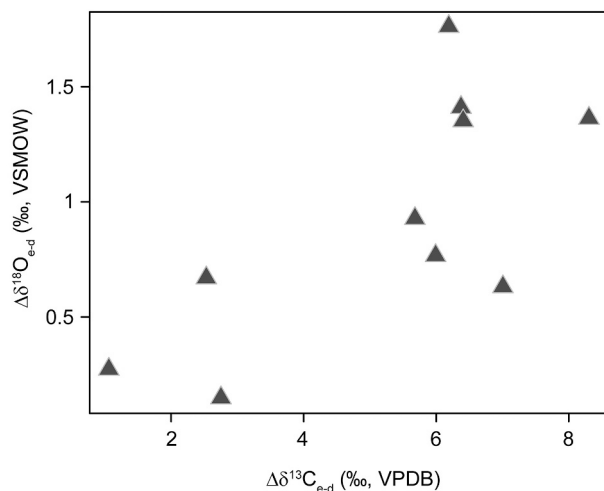


Fig. 10. Scatterplot of tooth-specific $\Delta\delta^{18}\text{O}_{\text{e-d}}$ and $\Delta\delta^{13}\text{C}_{\text{e-d}}$ values. Each point represents a single tooth ($n = 9$) of which both enamel and dentine samples were measured for their isotope content. These points depict the differences in oxygen and carbon values between enamel and dentine. Teeth that have higher/lower $\Delta\delta^{18}\text{O}_{\text{e-d}}$, generally have similar $\Delta\delta^{13}\text{C}_{\text{e-d}}$, suggesting that diagenesis at least was uniform across $\delta^{18}\text{O}$ and $\delta^{13}\text{C}$ values.

this bonebed. A clear (absolute) offset exists between the tooth-specific isotope content of enamel and dentine bioapatite for both oxygen (mean $\Delta\delta^{18}\text{O}_{\text{e-d}}$ of 0.87 ‰) and carbon (mean $\Delta\delta^{13}\text{C}_{\text{e-d}}$ of 5.54 ‰) for the *Triceratops* from the DTB (Fig. 10) (Stanton Thomas and Carlson, 2004). Hence, the observed isotope systematics of the DTB – especially the difference in enamel and dentine values – indicate some degree of isotopic alteration. Given the low concentration of dissolved inorganic carbon (DIC) compared to oxygen in fluids, the $\delta^{13}\text{C}$ values are generally less sensitive to isotopic alteration than the coexisting $\delta^{18}\text{O}$ values (c.f. van Baal et al., 2013). This could explain the larger spread in carbon data opposed to oxygen data observed in the dataset discussed here. However, although the absolute $\delta^{18}\text{O}$ values might be altered, the

relative variability is expected to be preserved within and between specimens.

The sedimentary matrix in the bonebed remained practically devoid of authigenic carbonates (on average 2.4 wt% CaCO_3 in the bonebed layer; Fig. 1C), providing an unlikely scenario for the uptake of secondary carbonates by the apatitic fossils. In this scenario, the pretreatment procedures aiming to remove secondary carbonates may have had adverse effects. While it might be too early to conclude that these *Triceratops* individuals are part of a biological (social) group, the rapid burial of multiple individuals suggest that the *Triceratops* lived and died at approximately the same time. In any event, they foraged and drank across similar geographical locations and have overlapping or homogenous diagenetic bone alterations due to the shared taphonomic history. This means that even partial preservation of an original isotope signature yields valuable information, as relative changes in $\delta^{18}\text{O}$ and $\delta^{13}\text{C}$ across the bonebed are comparable. While pretreatment protocols – and subsequent checks through C/P and FTIR – do provide shifts in isotope data, they remain inconsistent relating to the degree of diagenesis in this study. It agrees with the partial preservation of original isotope signatures, and we believe that the data compared and discussed for this specific bonebed provides meaningful results on dinosaur isotope systems.

5.3. Local water conditions and *Triceratops* habitat

Intra -and inter-tooth $\delta^{18}\text{O}$ variability of the DTB *Triceratops* is comparable to the variability in other dinosaurs as well as modern herbivorous mammals (Kohn et al., 1998; Stanton Thomas and Carlson, 2004). The differences in the $\delta^{18}\text{O}$ variability among the three taxa possibly reflects the relationship between the animal's physiology and ambient water, where lepisosteids and *Champsosaurus* $\delta^{18}\text{O}$ are more in isotopic equilibrium with their surrounding local water compared to free-roaming *Triceratops* $\delta^{18}\text{O}$, which shows the highest variability likely due to larger home ranges and access to different water sources.

Given their huge body volume, *Triceratops* can be considered at least gigantothermic and/or even endothermic, maintaining elevated body temperatures as proposed for other large-bodied non-avian dinosaurs (Amiot et al., 2006; Eagle et al., 2011; Erickson, 2014; Laskar et al.,

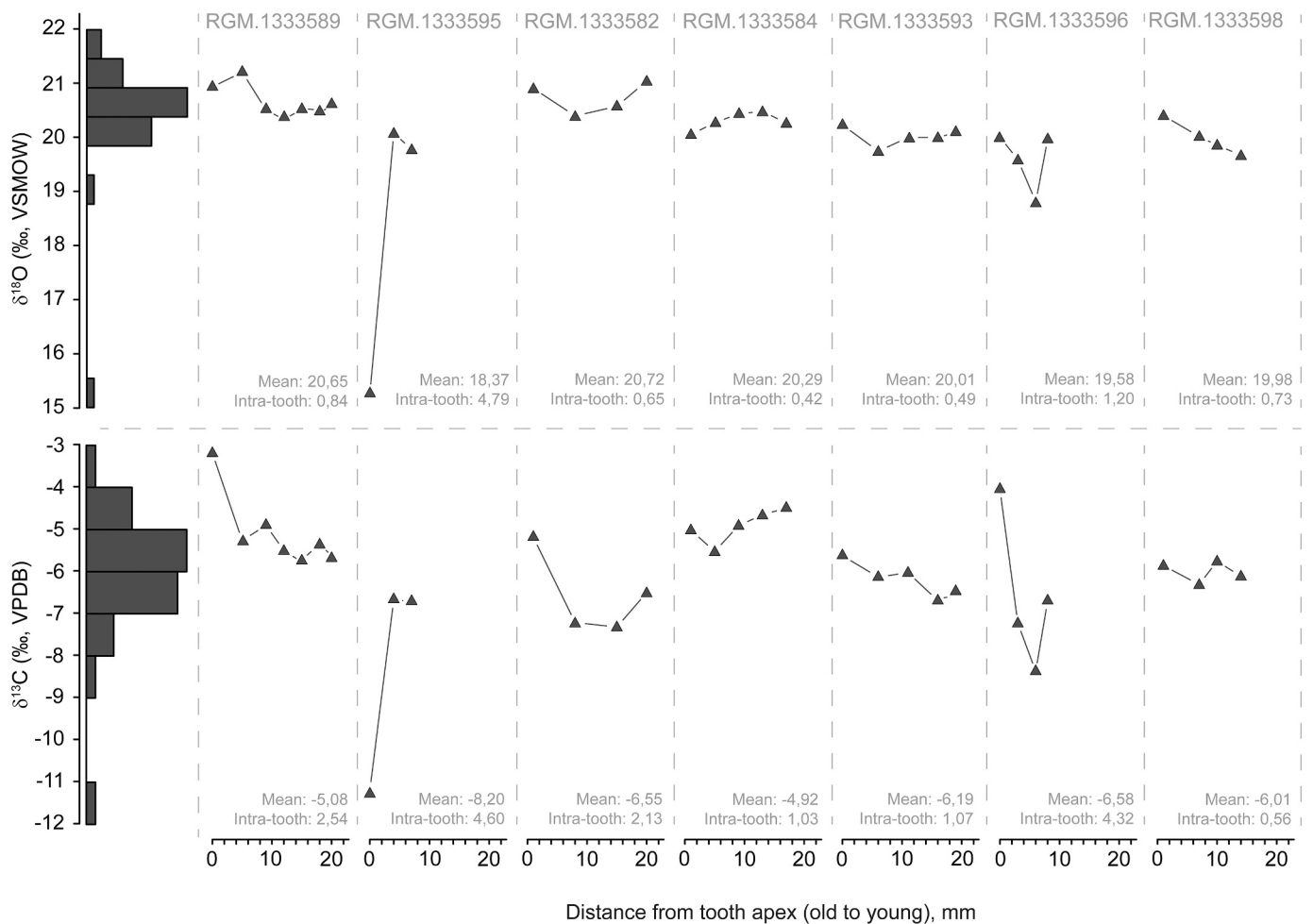


Fig. 11. $\delta^{18}\text{O}$ and $\delta^{13}\text{C}$ isotope values from the seven serially sampled *Triceratops* teeth. Note that, while the graphs are positioned in series, the teeth are considered to be independent and do not come from the same tooth battery or individual. Positioning of the graphs is based on random order. The distance from the tooth apex is oldest to youngest enamel. The histogram on the y-axis represents the total spread of the incremental data for $\delta^{18}\text{O}$ and $\delta^{13}\text{C}$.

2020). Based on $\delta^{18}\text{O}$ from phosphate and calculated $\delta^{18}\text{O}$ of body water, it has been shown that different taxa of dinosaurs – including ornithischians – show similar physiologies as mammals and are considered true endotherms (Amiot et al., 2006). This implies that *Triceratops* at least precipitated their apatite at elevated temperatures compared to ambient (air) temperatures. Therefore, the $\delta^{18}\text{O}$ variability in the *Triceratops* bioapatite likely reflects changes in the $\delta^{18}\text{O}$ of body water rather than body temperature.

The $\delta^{18}\text{O}$ of the body water of herbivores mainly depends on ingested drinking water and to a lesser extent on water that is ingested via plant food (Cerling and Harris, 1999), and is subsequently related to climatic parameters such as the $\delta^{18}\text{O}$ value of the local meteoric water, air temperature and humidity (Kohn et al., 1998; Kohn and Cerling, 2002; Fricke and Pearson, 2008). The $\delta^{18}\text{O}$ values in herbivores that drink large amounts of surface water and experience high water turnover rates – such as ungulates and elephants – generally track the $\delta^{18}\text{O}$ values of local water sources. On the contrary, if most of the ingested water is sourced from the plant food, the $\delta^{18}\text{O}$ in herbivores would be more strongly influenced by the local humidity (Kohn et al., 1996). Modelling experiments demonstrate that with increasing body size the amount of oxygen that is derived via the uptake of food and atmospheric O_2 decreases proportionally to the amount of oxygen taken up as free-drinking water (Bryant and Froelich, 1995). As a consequence, the $\delta^{18}\text{O}$ in teeth of *Triceratops* likely tracked changes in the $\delta^{18}\text{O}$ of the local surface drinking water ($\delta^{18}\text{O}_w$), and we posit that the $\delta^{18}\text{O}$ isotope signature in *Triceratops* enamel corroborates earlier inferences about the $\delta^{18}\text{O}$ body

water – which is a function of both local water sources and air temperature – and therefore informs on *Triceratops* behaviour and living environments.

Assuming a mammal-like physiology with relatively elevated and constant body temperatures for *Triceratops*, the $\delta^{18}\text{O}_w$ might be approximated from the *Triceratops* structural carbonate $\delta^{18}\text{O}$ ($\delta^{18}\text{O}_{sc}$) using the formula established for large, water-dependent herbivores by Hoppe (2006). All the *Triceratops* teeth of which enamel $\delta^{18}\text{O}$ was available produced an average $\delta^{18}\text{O}_w$ of -14.8‰ (total range -16.4 to -13.5‰ , $n = 12$) by inserting the corresponding $\delta^{18}\text{O}$ in formula [1]. This relatively low value coincides with inland freshwater systems ($\delta^{18}\text{O}_w < -11\text{‰}$) according to multiple independent $\delta^{18}\text{O}_w$ datasets on Late Cretaceous bivalves – specifically the Hell Creek and Lance Formation (Dettman and Lohmann, 2000; Tobin et al., 2014; Petersen et al., 2016). Bivalves store $\delta^{18}\text{O}$ in equilibrium with the surrounding water and have shown to express a bimodal distribution in their $\delta^{18}\text{O}$ signature (Tobin et al., 2014). Lower $\delta^{18}\text{O}$ values represent freshwater rivers while higher values may be associated with brackish to saltwater coastal floodplain settings (Petersen et al., 2016). This observation of lower oxygen values agrees with the sedimentological setting and hypothesized freshwater floodplain depositional environment for the Darnell *Triceratops* Bonebed.

Since the fossil remains did not undergo long-distance transport after death and deposition, the calculated $\delta^{18}\text{O}_w$ of -14.8‰ from formula [1] can be interpreted as the local hydrological conditions unique to this fossil assemblage, and – combined with the sedimentological context –

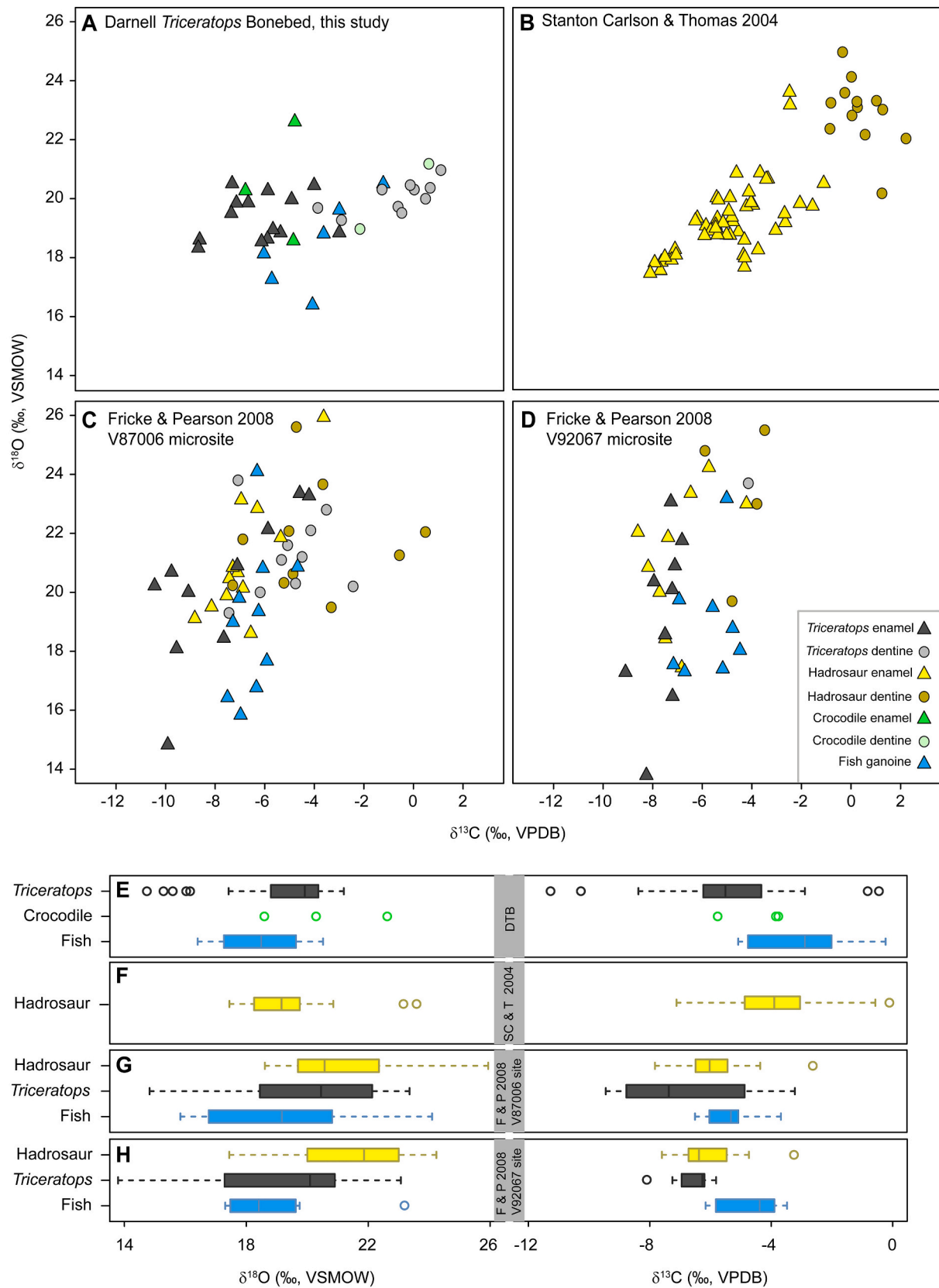


Fig. 12. Comparison of $\delta^{18}\text{O}$ and $\delta^{13}\text{C}$ data from this study with other contemporaneous Late Cretaceous dinosaur sites of which data was available (Fig. 1A). Upper part shows cross plots of four different dinosaur sites (A to D) and their respective $\delta^{18}\text{O}$ and $\delta^{13}\text{C}$ isotope systematics. Lower part focusses on the spread and range of the enamel $\delta^{18}\text{O}$ and $\delta^{13}\text{C}$ values of the same sites (E to H). Note the larger spread in the spatially less-constrained sites.

Table 1

Overview of carbonate/phosphorus (C/P) and IR-SF values from *Triceratops* enamel, dentine and bone samples. Enamel samples are represented by RGM.1333589, dentine samples are represented by RGM.1333596 and bone samples are represented by unnumbered cortical femur fragments from the Darnell *Triceratops* Bonebed.

Treatment strategy	C/P ratio	IR-SF
Enamel leached with 0.1 M acetic acid	0.22	3.76
Enamel leached with 1 M calcium acetate buffer	0.74	6.19
Enamel untreated	−0.87	1.23
Dentine leached with 0.1 M acetic acid	2.14	3.26
Dentine leached with 1 M calcium acetate buffer	1.02	3.40
Dentine untreated	2.01	3.43
Bone leached with 0.1 M acetic acid	1.55	2.72
Bone leached with 1 M calcium acetate buffer	1.45	2.19
Bone untreated	0.3	2.48

provides evidence that these dinosaurs lived in very close vicinity of fluvial settings. *Triceratops* most probably ingested drinking water from rivers and channels and foraged for food around these types of areas. Previous assumptions on *Triceratops* habitat show that they were often placed in more forested settings or open marsh/floodplain habitats based on $\delta^{18}\text{O}$ isotope signatures, while contemporaneous hadrosaurs would occupy these river settings more commonly (Fricke and Pearson, 2008). Similar observations have been reported by Lyson and Longrich (2011) who compared dinosaur taxa between mudstone and sandstone deposits from the Hell Creek Formation and other Maastrichtian-aged formations in North America. Mudstone deposits – which reflect floodplain settings – showed the highest representation of ceratopsian dinosaurs, suggesting that their preferred habitat lies in these types of areas. The DTB is interpreted as a floodplain (mudstone) deposit, closely associated with more inland freshwater environments opposed to brackish or saltwater coastal floodplains. Based on isotope data presented here, the *Triceratops* of the DTB allows to expand the previously assumed habitat range for this species. Instead, *Triceratops* was not restricted to specific habitats, but seems to have occupied a more diverse set of habitats than previously thought (see section 6.4 for more details).

Considering an intra-annual variability in the enamel bioapatite, the average $\delta^{18}\text{O}$ range within all incrementally sampled *Triceratops* teeth of 1.3 ‰ can serve as a proxy for seasonal shifts. Von Ebner line counts (Fig. 3) reveal that this observed variation spans ~90 days. This range is slightly lower than is observed for contemporaneous hadrosaurs from the Late Cretaceous that showed an average intra-tooth $\delta^{18}\text{O}$ value of 1.8 ‰ in incrementally sampled teeth (Stanton Thomas and Carlson, 2004). The relatively small variation in the observed $\delta^{18}\text{O}$ time series of single teeth of *Triceratops* is thus comparable to records from other dinosaur sites (Stanton Thomas and Carlson, 2004; Fricke and Pearson, 2008; Fricke et al., 2008) and modern herbivorous mammals (Kohn et al., 1998). Migrating dinosaurs may have spent their life in different environments resulting in variable isotope intake. On the other hand, they are expected to follow areas with ideal ambient temperature ranges and food sources, which is theorized to homogenize $\delta^{18}\text{O}$ isotopic – and seasonal – variability over time (Stanton Thomas and Carlson, 2004). However, considering the limited variability and presence of unique isotopic environments (Fricke et al., 2008), we argue that the $\delta^{18}\text{O}$ signature here represents local seasonal variation and/or movement within a home range, implying restricted migratory behaviour. This interpretation agrees with previous studies on hadrosaur migration, where it is postulated that Late Cretaceous hadrosaurs showed limited dispersal in relatively restricted home ranges (Fricke et al., 2009; Terrill et al., 2020; Cullen et al., 2020; Cullen et al., 2022).

5.4. Interactions during carbon uptake

Triceratops would have exclusively fed on C3 plants since there is no evidence for C4 plants from the Late Cretaceous. The average $\delta^{13}\text{C}$ of all

sampled *Triceratops* enamel is -5.4 ‰ (total $\delta^{13}\text{C}$ range -11.3 to -0.4 ‰). This represents the higher end of the distribution for modern C3 grazers and largely overlaps with mixed C3/C4 feeders. Notably, the *Triceratops* from the DTB show considerable overlap in their $\delta^{13}\text{C}$ signatures with other contemporaneous herbivorous dinosaurs (Stanton Thomas and Carlson, 2004; Fricke and Pearson, 2008). For putative C3 browsers, hadrosaurs from the Hell Creek Formation showed a comparably higher mean enamel $\delta^{13}\text{C}$ of -3.9 ‰ (Stanton Thomas and Carlson, 2004). Fricke and Pearson (2008) analysed five sites (within ~50 km proximity) from the Hell Creek Formation of southern North-Dakota and obtained similar mean $\delta^{13}\text{C}$ values for hadrosaurs and ceratopsians (Fig. 12). Corresponding mean hadrosaur enamel $\delta^{13}\text{C}$ is -5.9 ‰ with a range of -6.0 to -5.8 ‰, while mean ceratopsian enamel $\delta^{13}\text{C}$ was -6.3 ‰ and had a larger range of -8.1 to -3.9 ‰ (Fricke and Pearson, 2008). Thus, $\delta^{13}\text{C}$ data from these Late Cretaceous dinosaur sites show extensive overlap with each other, and all seem to point to a relatively high $\delta^{13}\text{C}$ value when compared to modern C3 feeders.

Differences in $\delta^{13}\text{C}$ of atmospheric CO_2 over geological time may have contributed to the observed higher dinosaur isotope signatures. However, during the Late Maastrichtian, the estimated $\delta^{13}\text{C}$ of atmospheric CO_2 was only slightly higher (-6.1 ‰ (Barral et al., 2017)) compared to more recent (pre-industrial) values (~ -6.5 ‰), and therefore cannot explain the significantly higher $\delta^{13}\text{C}$ observed in dinosaur bioapatite alone (Stanton Thomas and Carlson, 2004; Fricke and Pearson, 2008).

Preliminary analysis of macrofloral remains indicate that the DTB yielded relatively high amounts of gymnosperm fossils compared to angiosperms. It has been suggested that gymnosperms have more positive $\delta^{13}\text{C}$ values than angiosperms (by 2–3 ‰ (Hare and Laverne, 2021)), and recent studies have indicated that small but consistent offsets in $\delta^{13}\text{C}$ between different plant types may vary strongly depending both on the plant species and prevailing climatic and environmental conditions (e.g., up to 2–3 ‰ for halophytes (Wei et al., 2008; Sheldon et al., 2020; Hare and Laverne, 2021)). Although specific studies on *Triceratops* feeding are lacking, it is proposed that ceratopsians were able to efficiently process fibrous plant material such as gymnosperms using their sharp beak and tooth batteries (Ostrom, 1966; Mallon and Anderson, 2014). A diet shifted more towards gymnosperms and/or halophytes may have led to higher $\delta^{13}\text{C}$ values.

One other explanation for elevated $\delta^{13}\text{C}$ values is that *Triceratops* and other herbivorous dinosaurs possibly had different $\delta^{13}\text{C}$ fractionation offset between ingested plant food and their bioapatite. While the mean $\delta^{13}\text{C}$ fractionation for herbivore mammals is ~ 14 ‰ (Cerling and Harris, 1999), the fractionation factors cover a range from 10 ‰ to 15 ‰ among different taxa, presumably as a result of physiological and metabolic differences (Passey et al., 2005; Rey et al., 2020). Data on carbon fractionation in herbivorous reptiles is scarce but the existing literature shows that they have similar $\delta^{13}\text{C}$ isotopic offsets of ~ 12 ‰ between the ingested plant material and their bioapatite (Biasatti, 2004). However, these observations must be interpreted with care as isotope fractionation in marine reptiles is also affected by diving behaviour (McConnaughey et al., 1997; Biasatti, 2004; Schulp et al., 2013). Birds such as modern ratites have a similar degree of carbon fractionation with ranges comparable to those observed in herbivorous mammals (13 ‰ to 16 ‰ (Johnson et al., 1998; Ségalen and Lee-Thorp, 2009)).

Fricke et al. (2008) and Fricke and Pearson (2008) compared bulk sedimentary organic matter with the $\delta^{13}\text{C}$ of ceratopsian and hadrosaurs across a large range of Late Cretaceous dinosaur localities and inferred a $\delta^{13}\text{C}$ offset of ~ 18 ‰ between dinosaur bioapatite and corresponding organic matter (remnants of local plant material). Such offset is higher than the average ~ 14 ‰ for extant herbivores and would suggest a plant food $\delta^{13}\text{C}$ of -23.4 ‰ for the DTB *Triceratops* (mean enamel $\delta^{13}\text{C}$ of -5.4 ‰), which corresponds to the higher tail end of known modern C3 plant distributions (-35 ‰ to -22 ‰ (Kohn, 2010)). Carbon isotope data on Late Cretaceous herbivore dinosaurs consistently yield an offset of ~ 18 ‰ and numerous authors have postulated the idea of a dinosaur-

specific feeding physiology (Stanton Thomas and Carlson, 2004; Fricke et al., 2008; Fricke and Pearson, 2008; Tütken, 2011; Zhao et al., 2021).

While specialized digestive tracts as seen in ruminant mammals most probably did not evolve in dinosaurs (Smith et al., 2000), one can only speculate on ideas such as dinosaurs possessing single large-chambered stomachs in which food was digested over relatively longer periods (Hummel et al., 2008). In modern herbivores, the intraspecific differences in carbon fractionation partially result from differences in the gut microbiome and methane production by methanogens (Passey et al., 2005). Longer retention times of ingested food combined with a unique intestinal microbiome in dinosaurs could reasonably produce similar variations in carbon isotope systematics as found in modern herbivorous taxa. Additionally, recent research found a relationship between body size and enamel-diet $\delta^{13}\text{C}$ offsets in extant mammals, where smaller (micromammals) and larger (megaherbivores) taxa show a difference as much as 7 ‰ (Tejada-Lara et al., 2018). Non-avian dinosaurs being the largest terrestrial herbivores to have ever existed could equally show an offset higher than the average 14 ‰. Adding these animal-specific factors to the sum as well as the earlier proposed environmental factors – such as elevated $\delta^{13}\text{C}$ in atmospheric CO_2 and specific plant physiologies – may explain the observed elevated carbon isotope signature in herbivorous dinosaurs (Stanton Thomas and Carlson, 2004). Nevertheless, there is need for a better understanding of the interplay between extant animals, their environments and their food nutrients during incorporation and fixation of specific (carbon) isotope signals to provide unequivocal evidence regarding dinosaur physiology (Tejada et al., 2020).

5.5. Niche partitioning

Time-equivalent hadrosaurs and ceratopsians from the Hell Creek Formation have shown consistent differences in combined $\delta^{18}\text{O}$ and $\delta^{13}\text{C}$ values (Fricke and Pearson, 2008). These offsets were interpreted as niche partitioning, whereby relatively high $\delta^{18}\text{O}$ and $\delta^{13}\text{C}$ values are associated with open marsh settings and lower values represent more inland forested areas (Fricke and Pearson, 2008). Additionally, ceratopsians show relatively higher and lower $\delta^{13}\text{C}$ values than fish in marsh and forest settings, respectively (Fricke and Pearson, 2008). Interestingly, the mean $\delta^{18}\text{O}$ of 19.4 ‰ and mean $\delta^{13}\text{C}$ of -5.4 ‰ of the DTB *Triceratops* fall roughly between these two clusters, which may suggest that these *Triceratops* individuals had lived in a transitional area between more open marsh settings and inland forests, such as fluvial systems. Moreover, the spread of the *Triceratops* isotope data discussed here is relatively small which corroborates our interpretation of the DTB as a single event responsible for the death and rapid burial of a large group of *Triceratops*. This becomes especially evident when the DTB is compared to sites characterized by a diverse range of fossil material that is likely concentrated due to reworking, erosion and/or attritional processes over a longer time period (Fig. 1A). Earlier hypotheses on ornithischian niche partitioning and habitat occupation were based on isotope data sampled on isolated material from multiple taphonomically-concentrated sites (Pearson et al., 2002; Fricke and Pearson, 2008). While these sites provided a novel view into dinosaur ecosystems, comparison of these multiple individual sites reveal that there is still much isotopic overlap (i.e., higher spread) between hadrosaurs and ceratopsians, particularly when each site is plotted and evaluated separately (Fig. 12). Based on more narrow constrained bonebeds, such as the DTB discussed here, isotope data suggest that both taxa were coexisting to a larger degree than previously thought. Additionally, multi-taxon isotope analyses on other well-constrained Late Cretaceous floodplain systems revealed similar significant overlap between the isotope signatures of ornithischian dinosaurs overall (Cullen et al., 2020). It appears that niche partitioning – as preserved in the DTB – among large-bodied herbivorous dinosaurs is more complex than previously thought, if they were partitioning at all. These may include (a combination of) diet specialisation, feeding height stratification and temporal separation (e.g., seasonal changes in habitat use, diurnal vs. nocturnal), all of which may be

difficult to infer with currently available isotope analyses.

The DTB expands the envelope of herbivorous dinosaur niche partitioning (Fricke and Pearson, 2008; Lyson and Longrich, 2011), and might even suggest that niche partitioning happened to a significantly lesser degree, at least in this part of the Lance Formation. Instead, Late Cretaceous herbivores could have inhabited specific areas not based on spatial setting, but with competition as actual limiting factor. This line of reasoning does not limit a taxon to a specific habitat, but creates a dynamic system in which areas are inhabited based mainly on the presence of other taxa or even conspecifics. Isotopic research on wider set of local bonebeds could shed more light on this assumption.

Nevertheless, our results demonstrate the application of spatially well-constrained dinosaur sites in stable isotope research. Many earlier studies on dinosaur isotope systems are based on aforementioned (micro-)sites with generally poorly constrained depositional setting, diagenetic conditions, stratigraphy and taphonomy. These taphonomically-concentrated fossils provide a space- and time-averaged isotope signal of a specific ecosystem that creates an understanding of large-scale palaeo-ecosystem dynamics. On the other hand, the chemical fingerprint of bonebeds with well-constrained fossil material represents a more accurate baseline of the local ecology of that specific environment and/or species, such as the DTB studied here. Combining data from both types of assemblages helps in understanding more broader biological implications such as niche partitioning and animal movement.

6. Conclusion

Isotopic analysis of the Darnell *Triceratops* Bonebed in eastern Wyoming provides a unique window in studying dinosaur ecosystems of Late Cretaceous North America. There is a significant difference in the $\delta^{18}\text{O}$ and $\delta^{13}\text{C}$ values between the enamel and dentine of aquatic reptiles and *Triceratops* from the Darnell *Triceratops* Bonebed. These differences are markedly stronger for the $\delta^{13}\text{C}$ isotope system. Contrary to previous studies, bone showed less deviation from enamel than dentine, despite its more porous matrix. Moreover, pretreatment effects from leaching and oxidation on enamel, dentine, and bone returned ambiguous results. Diagenesis may have affected the studied material here, but these effects are expected to be uniform and thus the observed $\delta^{18}\text{O}$ and $\delta^{13}\text{C}$ isotope signatures allow for inferences on *Triceratops* palaeoecology. This is corroborated by the lack of authigenic carbonates in the organic-rich claystone embedding the fossils and the rapid burial of the well-preserved fossils by a very fine sandstone layer. This strengthens the notion that diagenetic overprint may vary per locality and should be checked on a case-by-case basis.

This study provides novel insights on *Triceratops* behaviour and ecology by examining the seasonal patterns in incrementally sampled $\delta^{18}\text{O}$ from tooth enamel. In addition, the $\delta^{13}\text{C}$ isotope signatures revealed possible feeding habits, and corroborate earlier observations of dinosaur-specific carbon fractionation rates. The stable isotope data from multiple sympatric species in a spatially and temporally well-constrained fossil assemblage allowed for a detailed assessment of a local Late Cretaceous ecosystem, that could be placed in the framework of previously studied dinosaur isotope systematics. The stable isotope dataset presented here shows both the importance and limitations of stable isotopes as local indicator of habitat and home ranges as opposed to time-averaged localities. Future stable isotope analyses on dinosaur remains should combine data from locally well-constrained sites and taphonomically-concentrated sites to better understand diet, habitat preferences, and possible niche partitioning in dinosaur (palaeo-) ecosystems.

Declaration of Competing Interest

The authors declare that they have no known competing financial interests or personal relationships that could have appeared to influence the work reported in this paper.

Data availability

The raw data used in this research can be found among the Supplementary data as Excel file.

Acknowledgements

We like to express our sincerest gratitude to Donley and Nancy Darnell for their hospitality and help during field seasons. Additionally, we like to thank our team of volunteers for their enthusiasm and efforts in recovering the fossil material. Thanks to Bouke Lacet (Faculty of Science, Earth Sciences, VU Amsterdam) for making the thin-sections and to Natasja den Ouden (Naturalis Biodiversity Center) for streamlining access to the material and handling of the destructive sampling requests. In addition, we owe gratitude to Martijn Guliker, Yasmin Grooters and their team of volunteers (Naturalis Biodiversity Center) for the preparation of the material presented in this study. We are further thankful for the technical support by Thom Claessen from Utrecht University, Faculty of Geosciences in Utrecht. Martine Hagen, Unze van Buuren, Maarten Prins en Kay Beets (VU Amsterdam) are thanked for their assistance during the laser-diffraction particle size and thermogravimetric analyses. Additionally, we like to thank Lisette Kootker from the VU Amsterdam for providing us with samples on modern human enamel. The project is funded by the Dutch Research Council (NWO) through ALW Open Programme (ALWOP.633). We like to acknowledge Dylan Bastiaans (PIMUZ, Switzerland) for his valuable contributions and input in developing the initial research plan. Furthermore, our gratitude goes towards the Mondriaan Fonds for their important contribution in sponsoring the field seasons. Last but not least, we like to thank the two anonymous reviewers and associated editor Howard Falcon-Lang for their time in carefully reading the manuscript and for providing insightful, constructive comments and suggestions that helped improve the manuscript.

Appendix A. Supplementary data

Supplementary data to this article can be found online at <https://doi.org/10.1016/j.palaeo.2022.111274>.

References

- Amiot, R., Lécuyer, C., Buffetaut, E., Fluteau, F., Legendre, S., Martineau, F., 2004. Latitudinal temperature gradient during the cretaceous Upper Campanian-Middle Maastrichtian: $\delta^{18}\text{O}$ record of continental vertebrates. *Earth Planet. Sci. Lett.* 226 (1–2), 255–272.
- Amiot, R., Lécuyer, C., Buffetaut, E., Escarguel, G., Fluteau, F., Martineau, F., 2006. Oxygen isotopes from biogenic apatites suggest widespread endothermy in cretaceous dinosaurs. *Earth Planet. Sci. Lett.* 246 (1–2), 41–54.
- Amiot, R., Buffetaut, E., Lécuyer, C., Wang, X., Boudad, L., Ding, Z., Fourel, F., Hutt, S., Martineau, F., Medeiros, M.A., Mo, J., Simon, L., Suteethorn, V., Sweetman, S., Tong, H., Zhang, F., Zhou, Z., 2010. Oxygen isotope evidence for semi-aquatic habits among spinosaurid theropods. *Geology* 38 (2), 139–142.
- Assonov, S., Groening, M., Fajgelj, A., Hélie, J.F., Hillaire-Marcel, C., 2020. Preparation and characterisation of IAEA-603, a new primary reference material aimed at the VPDB scale realisation for $\delta^{13}\text{C}$ and $\delta^{18}\text{O}$ determination. *Rapid Commun. Mass Spectrom.* 34 (20), e8867.
- van Baal, R.R., Janssen, R., Van der Lubbe, H.J.L., Schulp, A.S., Jagt, J.W., Vonhof, H.B., 2013. Oxygen and carbon stable isotope records of marine vertebrates from the type Maastrichtian, the Netherlands and Northeast Belgium (Late Cretaceous). *Palaeogeogr. Palaeoclimatol. Palaeoecol.* 392, 71–78.
- Balter, V., 2001. Were Neandertalians essentially carnivores? Sr and Ba preliminary results of the mammalian palaeobiocoenosis of Saint-Césaire. *Compt. Rend. Acad. Sci. Ser. Fascic. Asci. Terre Planètes* 332, 59–65.
- Barbour, M.M., 2007. Stable oxygen isotope composition of plant tissue: a review. *Funct. Plant Biol.* 34 (2), 83–94.
- Barral, A., Gomez, B., Legendre, S., Lécuyer, C., 2017. Evolution of the carbon isotope composition of atmospheric CO_2 throughout the cretaceous. *Palaeogeogr. Palaeoclimatol. Palaeoecol.* 471, 40–47.
- Barrick, R.E., 1998. Isotope paleobiology of the vertebrates: ecology, physiology, and diagenesis, 4, 101–137. The Paleontological Society Papers.
- Bartos, T.T., Galloway, D.L., Hallberg, L.L., Deschene, M., Diehl, S.F., Davidson, S.L., 2021. Geologic and Hydrogeologic Characteristics of the White River Formation, Lance Formation, and Fox Hills Sandstone, Northern Greater Denver Basin, Southeastern Laramie County, Wyoming (No. 2021-5020). US Geological Survey.
- Bastiaans, D., Trapman, T., Guliker, M., Kaskes, P., Schulp, A., 2016. Multigenerational assemblage of Triceratops from the Newcastle area, Wyoming, USA – An in-depth analysis of cranial and post-cranial ontogenesis. In: 76th Annual Meeting of the Society of Vertebrate Paleontology (SVP), p. 94.
- Beasley, M.M., Bartelink, E.J., Taylor, L., Miller, R.M., 2014. Comparison of transmission FTIR, ATR, and DRIFT spectra: implications for assessment of bone biapatite diagenesis. *J. Archaeol. Sci.* 46, 16–22.
- Berna, F., Matthews, A., Weiner, S., 2004. Solubilities of bone mineral from archaeological sites: the recrystallization window. *J. Archaeol. Sci.* 31 (7), 867–882.
- Biasatti, D.M., 2004. Stable carbon isotopic profiles of sea turtle humeri: implications for ecology and physiology. *Palaeogeogr. Palaeoclimatol. Palaeoecol.* 206 (3–4), 203–216.
- Brown, C.M., Campione, N.E., Mantilla, G.P.W., Evans, D.C., 2022. Size-driven preservational and macroecological biases in the latest Maastrichtian terrestrial vertebrate assemblages of North America. *Paleobiology* 48 (2), 210–238.
- Bryant, J.D., Froelich, P.N., 1995. A model of oxygen isotope fractionation in body water of large mammals. *Geochim. Cosmochim. Acta* 59 (21), 4523–4537.
- de Buffrénil, V., de Ricqlès, A.J., Zylberberg, L., Padian, K., 2021. In: *Vertebrate Skeletal Histology and Paleohistology*. CRC Press, pp. 229–246.
- Burgener, L., Hyland, E., Griffith, E., Mitášová, H., Zanno, L.E., Gates, T.A., 2021. An extreme climate gradient-induced ecological regionalization in the Upper cretaceous Western Interior Basin of North America. *GSA Bulletin* 133 (9–10), 2125–2136.
- Burns, C.E., Mountney, N.P., Hodgson, D.M., Colombero, L., 2017. Anatomy and dimensions of fluvial crevasse-splay deposits: examples from the cretaceous Castlegate Sandstone and Neslen Formation, Utah, USA. *Sediment. Geol.* 351, 21–35.
- Carlson, S.J., 1990. Vertebrate dental structures. Skeletal biomineralization: patterns, processes and evolutionary trends 5, 235–260.
- Cerling, T.E., Harris, J.M., 1999. Carbon isotope fractionation between diet and biapatite in ungulate mammals and implications for ecological and paleoecological studies. *Oecologia* 120 (3), 347–363.
- Cerling, T.E., Harris, J.M., MacFadden, B.J., Leakey, M.G., Quade, J., Eisenmann, V., Ehleringer, J.R., 1997. Global vegetation change through the Miocene/Pliocene boundary. *Nature* 389 (6647), 153–158.
- Coplen, T.B., 1988. Normalization of oxygen and hydrogen isotope data. *Chem. Geol.* 72 (4), 293–297.
- Crystal, V.F., Evans, E.S., Fricke, H., Miller, I.M., Sertich, J.J., 2019. Late cretaceous fluvial hydrology and dinosaur behavior in southern Utah, USA: Insights from stable isotopes of biogenic carbonate. *Palaeogeogr. Palaeoclimatol. Palaeoecol.* 516, 152–165.
- Cullen, T.M., Longstaffe, F.J., Wortmann, U.G., Huang, L., Fanti, F., Goodwin, M.B., Ryan, M.J., Evans, D.C., 2020. Large-scale stable isotope characterization of a late cretaceous dinosaur-dominated ecosystem. *Geology* 48 (6), 546–551.
- Cullen, T.M., Zhang, S., Spencer, J., Cousins, B., 2022. Sr-O-C isotope signatures reveal herbivore niche-partitioning in a cretaceous ecosystem. *Palaeontology* 65 (2), e12591.
- Dansgaard, W., 1964. Stable isotopes in precipitation. *Tellus* 16 (4), 436–468.
- Dettman, D.L., Lohmann, K.C., 2000. Oxygen isotope evidence for high-altitude snow in the Laramide Rocky Mountains of North America during the late cretaceous and Paleogene. *Geology* 28 (3), 243–246.
- Dufour, E., Holmden, C., Van Neer, W., Zazzo, A., Patterson, W.P., Degryse, P., Keppens, E., 2007. Oxygen and strontium isotopes as provenance indicators of fish at archaeological sites: the case study of Sagalassos, SW Turkey. *J. Archaeol. Sci.* 34 (8), 1226–1239.
- Eagle, R.A., Tütken, T., Martin, T.S., Tripathi, A.K., Fricke, H.C., Connely, M., Cifelli, R.L., Eiler, J.M., 2011. Dinosaur body temperatures determined from isotopic (^{13}C – ^{18}O) ordering in fossil biominerals. *Science* 333 (6041), 443–445.
- Vander Zanden, Clayton, M.K., Moody, E.K., Solomon, C.T., Weidel, B.C., 2015. Stable isotope turnover and half-life in animal tissues: a literature synthesis. *PLoS one* 10 (1), e0116182.
- von Ebner, V., 1902. Histologie der Zähne mit Einschluß der Histogenese. In: Scheff, J. (Ed.), *Handbuch der Zahnheilkunde*. Holder, Wein, pp. 243–299.
- Erickson, G.M., 1996. Incremental lines of von Ebner in dinosaurs and the assessment of tooth replacement rates using growth line counts. *Proc. Natl. Acad. Sci.* 93 (25), 14623–14627.
- Erickson, G.M., 2014. On dinosaur growth. *Annu. Rev. Earth Planet. Sci.* 42, 675–697.
- Erickson, G.M., Sidebottom, M.A., Kay, D.L., Turner, K.T., Ip, N., Norell, M.A., Sawyer, W. G., Erick, B.A., 2015. Wear biomechanics in the slicing dentition of the giant horned dinosaur Triceratops. *Sci. Adv.* 1 (5), e1500055.
- Erickson, G.M., Zelenitsky, D.K., Kay, D.L., Norell, M.A., 2017. Dinosaur incubation periods directly determined from growth-line counts in embryonic teeth show reptilian-grade development. *Proc. Natl. Acad. Sci.* 114 (3), 540–545.
- Farke, A.A., Wolff, E.D., Tanke, D.H., 2009. Evidence of combat in Triceratops. *PLoS One* 4 (1), e4252.
- Fastovsky, D.E., Bercovici, A., 2016. The Hell Creek Formation and its contribution to the Cretaceous-Paleogene extinction: a short primer. *Cretac. Res.* 57, 368–390.
- FitzGerald, C.M., 1998. Do enamel microstructures have regular time dependency? Conclusions from the literature and a large-scale study. *J. Hum. Evol.* 35 (4–5), 371–386.
- Fricke, H.C., Rogers, R.R., 2000. Multiple taxon–multiple locality approach to providing oxygen isotope evidence for warm-blooded theropod dinosaurs. *Geology* 28 (9), 799–802.
- Frederickson, J.A., Engel, M.H., Cifelli, R.L., 2020. Ontogenetic dietary shifts in *Deinonychus antirrhopus* (Theropoda; Dromaeosauridae): Insights into the ecology

- and social behavior of raptorial dinosaurs through stable isotope analysis. *Palaeogeogr. Palaeoclimatol. Palaeoecol.* 552, 109780.
- Fricke, H.C., Pearson, D.A., 2008. Stable isotope evidence for changes in dietary niche partitioning among hadrosaurian and ceratopsian dinosaurs of the Hell Creek Formation North Dakota. *Paleobiology* 34 (4), 534–552.
- Fricke, H.C., Rogers, R.R., Backlund, R., Dwyer, C.N., Echt, S., 2008. Preservation of primary stable isotope signals in dinosaur remains, and environmental gradients of the late cretaceous of Montana and Alberta. *Palaeogeogr. Palaeoclimatol. Palaeoecol.* 266 (1–2), 13–27.
- Fricke, H.C., Rogers, R.R., Gates, T.A., 2009. Hadrosaurid migration: inferences based on stable isotope comparisons among late cretaceous dinosaur localities. *Paleobiology* 35 (2), 270–288.
- Garvie-Lok, S.J., Varney, T.L., Katzenberg, M.A., 2004. Preparation of bone carbonate for stable isotope analysis: the effects of treatment time and acid concentration. *J. Archaeol. Sci.* 31 (6), 763–776.
- Glimcher, M.J., 2006. Bone: nature of the calcium phosphate crystals and cellular, structural, and physical chemical mechanisms in their formation. *Rev. Mineral. Geochem.* 64 (1), 223–282.
- Goedert, J., Amiot, R., Boudad, L., Buffetaut, E., Fourrel, F., Godefroit, P., Kusuhashi, N., Suteethorn, V., Tong, H., Watabe, M., Lécuyer, C., 2016. Preliminary investigation of seasonal patterns recorded in the oxygen isotope compositions of theropod dinosaur tooth enamel. *Palaios* 31 (1), 10–19.
- Goodwin, M.B., Clemens, W.A., Horner, J.R., Padian, K., 2006. The smallest known Triceratops skull: new observations on ceratopsid cranial anatomy and ontogeny. *J. Vertebr. Paleontol.* 26 (1), 103–112.
- Goodwin, M.B., Horner, J.R., Ryan, M., Chinnery-Algeier, B.J., Eberth, D.A., 2010. Historical collecting bias and the fossil record of Triceratops in Montana. In: *New Perspectives on Horned Dinosaurs. The Royal Tyrrell Museum Ceratopsian Symposium*. Indiana University Press, Bloomington, Indiana, pp. 551–563.
- Graven, H., Keeling, R.F., Rogelj, J., 2020. Changes to carbon isotopes in atmospheric CO₂ over the industrial era and into the future. *Glob. Biogeochem. Cycles* 34 (11), e2019GB006170.
- Hassler, A., Martin, J.E., Amiot, R., Tacail, T., Godet, F.A., Allain, R., Balter, V., 2018. Calcium isotopes offer clues on resource partitioning among cretaceous predatory dinosaurs. *Proc. R. Soc. B Biol. Sci.* 285 (1876), 20180197.
- Hare, V.J., Laverne, A., 2021. Differences in carbon isotope discrimination between angiosperm and gymnosperm woody plants, and their geological significance. *Geochim. Cosmochim. Acta* 300, 215–230.
- Herwartz, D., Tütken, T., Jochum, K.P., Sander, P.M., 2013. Rare earth element systematics of fossil bone revealed by LA-ICPMS analysis. *Geochim. Cosmochim. Acta* 103, 161–183.
- Herwartz, D., Tütken, T., Münker, C., Jochum, K.P., Stoll, B., Sander, P.M., 2011. Timescales and mechanisms of REE and Hf uptake in fossil bones. *Geochim. Cosmochim. Acta* 75 (1), 82–105.
- Hobson, K.A., Wassenaar, L.I., 2018. *Tracking animal migration with stable isotopes*. Academic Press.
- Hoppe, K.A., 2006. Correlation between the oxygen isotope ratio of north american bison teeth and local waters: Implication for paleoclimatic reconstructions. *Earth Planet. Sci. Lett.* 244 (1–2), 408–417.
- Horner, J.R., De Ricqlès, A., Padian, K., 2000. Long bone histology of the hadrosaurid dinosaur *Maiaasaura peeblesorum*: growth dynamics and physiology based on an ontogenetic series of skeletal elements. *J. Vertebr. Paleontol.* 20 (1), 115–129.
- Horner, J.R., Goodwin, M.B., 2006. Major cranial changes during Triceratops ontogeny. *Proc. R. Soc. B Biol. Sci.* 273 (1602), 2757–2761.
- Hummel, J., Gee, C.T., Südekum, K.H., Sander, P.M., Nogge, G., Clauss, M., 2008. In vitro digestibility of fern and gymnosperm foliage: implications for sauroid feeding ecology and diet selection. *Proc. R. Soc. B Biol. Sci.* 275 (1638), 1015–1021.
- Hwang, S.H., 2005. Phylogenetic patterns of enamel microstructure in dinosaur teeth. *J. Morphol.* 266 (2), 208–240.
- Illies, M.M.C., Fowler, D.W., 2020. Triceratops with a kink: Co-ossification of five distal caudal vertebrae from the Hell Creek Formation of North Dakota. *Cretac. Res.* 108, 104355.
- Janssen, R., Joordens, J.C., Koutamanis, D.S., Puspaningrum, M.R., de Vos, J., Van Der Lubbe, J.H., Reijmer, J.J.G., Hampe, O., Vonhof, H.B., 2016. Tooth enamel stable isotopes of Holocene and Pleistocene fossil fauna reveal glacial and interglacial paleoenvironments of hominins in Indonesia. *Quat. Sci. Rev.* 144, 145–154.
- Johnson, B.J., Fogel, M.L., Miller, G.H., 1998. Stable isotopes in modern ostrich eggshell: a calibration for paleoenvironmental applications in semi-arid regions of southern Africa. *Geochim. Cosmochim. Acta* 62 (14), 2451–2461.
- Johnson, K.R., Nichols, D.J., Hartman, J.H., 2002. Hell Creek Formation: a 2001 synthesis. *Geol. Soc. Am. Spec. Pap.* 361, 503–510.
- Kaskes, P., Portanger, L.A., Schulp, A.S., 2016. Unravelling the history of a unique Triceratops graveyard from eastern Wyoming, USA. In: *XIV Annual Meeting of the European Association of Vertebrate Palaeontologists*, p. 192.
- Kaskes, P., Bastiaans, D., Verhage, O., de Rooij, J., Guliker, M., Schulp, A.S., 2019. Taphonomy of a unique multigenerational Triceratops bonebed from eastern Wyoming (USA): New insights from a multi-proxy perspective. In: *European Association of Vertebrate Paleontologists: XVII Annual Meeting*, p. 54.
- Kendall, C., Eriksen, A.M.H., Kontopoulos, I., Collins, M.J., Turner-Walker, G., 2018. Diagenesis of archaeological bone and tooth. *Palaeogeogr. Palaeoclimatol. Palaeoecol.* 491, 21–37.
- Kim, S.T., Coplen, T.B., Horita, J., 2015. Normalization of stable isotope data for carbonate minerals: implementation of IUPAC guidelines. *Geochim. Cosmochim. Acta* 158.
- Koch, P.L., Tuross, N., Fogel, M.L., 1997. The effects of sample treatment and diagenesis on the isotopic integrity of carbonate in biogenic hydroxylapatite. *J. Archaeol. Sci.* 24 (5), 417–429.
- Koch, P.L., 1998. Isotopic reconstruction of past continental environments. *Annu. Rev. Earth Planet. Sci.* 26 (1), 573–613.
- Kohn, M.J., 2010. Carbon isotope compositions of terrestrial C3 plants as indicators of (paleo) ecology and (paleo) climate. *Proc. Natl. Acad. Sci.* 107 (46), 19691–19695.
- Kohn, M.J., Cerling, T.E., 2002. Stable isotope compositions of biological apatite. *Rev. Mineral. Geochem.* 48 (1), 455–488.
- Kohn, M.J., Schoeninger, M.J., Valley, J.W., 1996. Herbivore tooth oxygen isotope compositions: effects of diet and physiology. *Geochim. Cosmochim. Acta* 60 (20), 3889–3896.
- Kohn, M.J., Schoeninger, M.J., Valley, J.W., 1998. Variability in oxygen isotope compositions of herbivore teeth: reflections of seasonality or developmental physiology? *Chem. Geol.* 152 (1–2), 97–112.
- Konert, M., Vandenbergh, J.E.F., 1997. Comparison of laser grain size analysis with pipette and sieve analysis: a solution for the underestimation of the clay fraction. *Sedimentology* 44 (3), 523–535.
- Krueger, H.W., 1991. Exchange of carbon with biological apatite. *J. Archaeol. Sci.* 18 (3), 355–361.
- Laskar, A.H., Mohabey, D., Bhattacharya, S.K., Liang, M.C., 2020. Variable thermoregulation of late cretaceous dinosaurs inferred by clumped isotope analysis of fossilized eggshell carbonates. *Heliyon* 6 (10), e05265.
- Layman, C.A., Araujo, M.S., Boucek, R., Hammerschlag-Peyer, C.M., Harrison, E., Jud, Z. R., Matich, P., Rosenblatt, A.E., Vaudo, J.J., Yeager, L.A., Post, D.M., Bearhop, S., 2012. Applying stable isotopes to examine food-web structure: an overview of analytical tools. *Biol. Rev.* 87 (3), 545–562.
- Le Boedec, K., 2016. Sensitivity and specificity of normality tests and consequences on reference interval accuracy at small sample size: a computer-simulation study. *Vet. Clin. Pathol.* 45 (4), 648–656.
- Lee-Thorp, J.A., 2002. Preservation of biogenic carbon isotopic signals in Plio-Pleistocene bone and tooth mineral. In: *Biogeochemical Approaches to Paleodietary Analysis*. Springer, Boston, MA, pp. 89–115.
- Lee-Thorp, J.A., Van der Merwe, N.J., 1987. Carbon isotope analysis of fossil bone apatite. *S. Afr. J. Sci.* 83 (11), 712–715.
- Lee-Thorp, J.A., van der Merwe, N.J., 1991. Aspects of the chemistry of modern and fossil biological apatites. *J. Archaeol. Sci.* 18 (3), 343–354.
- Line, S.R., 2000. Incremental markings of enamel in ectothermal vertebrates. *Arch. Oral Biol.* 45 (5), 363–368.
- Longrich, N.R., Field, D.J., 2012. *Torosaurus* is not *Triceratops*: ontogeny in chasmosaurine ceratopsids as a case study in dinosaur taxonomy. *PloS One* 7 (2), e32623.
- Lyson, T.R., Longrich, N.R., 2011. Spatial niche partitioning in dinosaurs from the latest cretaceous (Maastrichtian) of North America. *Proc. R. Soc. B Biol. Sci.* 278 (1709), 1158–1164.
- Mallon, J.C., Anderson, J.S., 2014. Implications of beak morphology for the evolutionary paleoecology of the megaherbivorous dinosaurs from the Dinosaur Park Formation (upper Campanian) of Alberta, Canada. *Palaeogeogr. Palaeoclimatol. Palaeoecol.* 394, 29–41.
- Mathews, J.C., Brusatte, S.L., Williams, S.A., Henderson, M.D., 2009. The first Triceratops bonebed and its implications for gregarious behavior. *J. Vertebr. Paleontol.* 29 (1), 286–290.
- McConaughy, T.A., Burdett, J., Whelan, J.F., Paull, C.K., 1997. Carbon isotopes in biological carbonates: respiration and photosynthesis. *Geochim. Cosmochim. Acta* 61 (3), 611–622.
- Nielsen-Marsh, C.M., Hedges, R.E., 2000. Patterns of diagenesis in bone I: the effects of site environments. *J. Archaeol. Sci.* 27 (12), 1139–1150.
- Njau, J.K., Blumenshine, R.J., 2006. A diagnosis of crocodile feeding traces on larger mammal bone, with fossil examples from the Plio-Pleistocene Olduvai Basin, Tanzania. *J. Human Evol.* 50 (2), 142–162.
- O'Meara, R.N., Dirks, W., Martinelli, A.G., 2018. Enamel formation and growth in non-mammalian cynodonts. *R. Soc. Open Sci.* 5 (5), 172293.
- Ostrom, J.H., 1966. Functional morphology and evolution of the ceratopsian dinosaurs. *Evolution* 290–308.
- Ostrom, P.H., Macko, S.A., Engel, M.H., Russell, D.A., 1993. Assessment of trophic structure of cretaceous communities based on stable nitrogen isotope analyses. *Geology* 21 (6), 491–494.
- Passey, B.H., Robinson, T.F., Ayliffe, L.K., Cerling, T.E., Sponheimer, M., Dearing, M.D., Roeder, B.L., Ehleringer, J.R., 2005. Carbon isotope fractionation between diet, breath CO₂, and bioapatite in different mammals. *J. Archaeol. Sci.* 32 (10), 1459–1470.
- Pearson, D.A., Schaefer, T., Johnson, K.R., Nichols, D.J., Hunter, J.P., 2002. Vertebrate biostratigraphy of the Hell Creek formation in southwestern North Dakota and northwestern South Dakota. *Geol. Soc. Am. Spec. Pap.* 361, 145–167.
- Pecquerie, L., Nisbet, R.M., Fablet, R., Lorrain, A., Kooijman, S.A., 2010. The impact of metabolism on stable isotope dynamics: a theoretical framework. *Phil. Trans. Royal Soc. B Biol. Sci.* 365 (1557), 3455–3468.
- Pellegrini, M., Snoeck, C., 2016. Comparing bioapatite carbonate pre-treatments for isotopic measurements: part 2—Impact on carbon and oxygen isotope compositions. *Chem. Geol.* 420, 88–96.
- Pellegrini, M., Lee-Thorp, J.A., Donahue, R.E., 2011. Exploring the variation of the $\delta^{18}\text{O}$ and $\delta^{18}\text{O}$ relationship in enamel increments. *Palaeogeogr. Palaeoclimatol. Palaeoecol.* 310 (1–2), 71–83.
- Petersen, S.V., Tabor, C.R., Lohmann, K.C., Poulsen, C.J., Meyer, K.W., Carpenter, S.J., Erickson, J.M., Matsunaga, K.K.S., Smith, S.Y., Sheldon, N.D., 2016. Temperature

- and salinity of the Late Cretaceous western interior seaway. *Geology* 44 (11), 903–906.
- Rey, K., Amiot, R., Fourel, F., Abdala, F., Fluteau, F., Jalil, N.E., Liu, J., Rubidge, B.S., Smith, R.M.H., Steyer, J.S., Viglietti, P.A., Wang, X., Lecuyer, C., 2017. Oxygen isotopes suggest elevated thermometabolism within multiple Permo-Triassic therapsid clades. *elife* 6, e28589.
- Rey, K., Day, M.O., Amiot, R., Fourel, F., Luyt, J., Lecuyer, C., Rubidge, B.S., 2020. Stable isotopes ($\delta^{18}\text{O}$ and $\delta^{13}\text{C}$) give new perspective on the ecology and diet of *Endothiodon bathystoma* (Therapsida, Dicynodontia) from the late Permian of the South African Karoo Basin. *Palaeogeogr. Palaeoclimatol. Palaeoecol.* 556, 109882.
- Sage, R.F., 2004. The evolution of C4 photosynthesis. *New Phytol.* 161 (2), 341–370.
- Sander, P.M., 1999. The microstructure of reptilian tooth enamel: terminology, function, and phylogeny. *F. Pfeil*.
- Scannella, J.B., Fowler, D.W., Goodwin, M.B., Horner, J.R., 2014. Evolutionary trends in Triceratops from the Hell Creek formation, Montana. *Proc. Natl. Acad. Sci.* 111 (28), 10245–10250.
- Schulp, A.S., Vonnhof, H.B., Van der Lubbe, J.H.J.L., Janssen, R., Van Baal, R.R., 2013. On diving and diet: resource partitioning in type-Maastrichtian mosasaurs. *Neth. J. Geosci.* 92 (2–3), 165–170.
- Schwarz, H.P., 2015, October.. The ultrastructure of bone as revealed in electron microscopy of ion-milled sections. In: *Seminars in Cell & Developmental Biology*, Vol. 46. Academic Press, pp. 44–50.
- Ségalen, L., Lee-Thorp, J.A., 2009. Palaeoecology of late early Miocene fauna in the Namib based on $^{13}\text{C}/^{12}\text{C}$ and $^{18}\text{O}/^{16}\text{O}$ ratios of tooth enamel and ratite eggshell carbonate. *Palaeogeogr. Palaeoclimatol. Palaeoecol.* 277 (3–4), 191–198.
- Sheldon, N.D., Smith, S.Y., Stein, R., Ng, M., 2020. Carbon isotope ecology of gymnosperms and implications for paleoclimatic and paleoecological studies. *Glob. Planet. Chang.* 184, 103060.
- Smith, T.M., 2006. Experimental determination of the periodicity of incremental features in enamel. *J. Anat.* 208 (1), 99–113.
- Smith, B.N., Epstein, S., 1971. Two categories of $^{13}\text{C}/^{12}\text{C}$ ratios for higher plants. *Plant Physiol.* 47 (3), 380–384.
- Smith, D.M., Grasty, R.C., Theodosiou, N.A., Tabin, C.J., Nascone-Yoder, N.M., 2000. Evolutionary relationships between the amphibian, avian, and mammalian stomachs. *Evol. Dev.* 2 (6), 348–359.
- Snoeck, C., Pellegrini, M., 2015. Comparing bioapatite carbonate pre-treatments for isotopic measurements: part 1—Impact on structure and chemical composition. *Chem. Geol.* 417, 394–403.
- Stanton Thomas, K.J., Carlson, S.J., 2004. Microscale $\delta^{18}\text{O}$ and $\delta^{13}\text{C}$ isotopic analysis of an ontogenetic series of the hadrosaurid dinosaur *Edmontosaurus*: implications for physiology and ecology. *Palaeogeogr. Palaeoclimatol. Palaeoecol.* 206 (3–4), 257–287.
- Straight, W.H., Barrick, R.E., Eberth, D.A., 2004. Reflections of surface water, seasonality and climate in stable oxygen isotopes from tyrannosaurid tooth enamel. *Palaeogeogr. Palaeoclimatol. Palaeoecol.* 206 (3–4), 239–256.
- Tafforeau, P., Bentalab, L., Jaeger, J.J., Martin, C., 2007. Nature of laminations and mineralization in rhinoceros enamel using histology and X-ray synchrotron microtomography: potential implications for palaeoenvironmental isotopic studies. *Palaeogeogr. Palaeoclimatol. Palaeoecol.* 246 (2–4), 206–227.
- Taiz, L., Zeiger, E., Møller, I.M., Murphy, A., 2015. *Plant physiology and development* (No. Ed. 6). Sinauer Associates Incorporated.
- Tejada-Lara, J.V., MacFadden, B.J., Bermudez, L., Rojas, G., Salas-Gismondi, R., Flynn, J.J., 2018. Body mass predicts isotope enrichment in herbivorous mammals. *Proc. R. Soc. B* 285 (1881), 20181020.
- Tejada, J.V., Flynn, J.J., Antoine, P.O., Pacheco, V., Salas-Gismondi, R., Cerling, T.E., 2020. Comparative isotope ecology of western amazonian rainforest mammals. *Proc. Natl. Acad. Sci.* 117 (42), 26263–26272.
- Terrill, D.F., Henderson, C.M., Anderson, J.S., 2020. New application of strontium isotopes reveals evidence of limited migratory behaviour in late cretaceous hadrosaurs. *Biol. Lett.* 16 (3), 20190930.
- Thompson, T.J.U., Gauthier, M., Islam, M., 2009. The application of a new method of Fourier Transform infrared Spectroscopy to the analysis of burned bone. *J. Archaeol. Sci.* 36 (3), 910–914.
- Tieszen, L.L., 1991. Natural variations in the carbon isotope values of plants: implications for archaeology, ecology, and paleoecology. *J. Archaeol. Sci.* 18 (3), 227–248.
- Tobin, T.S., Wilson, G.P., Eiler, J.M., Hartman, J.H., 2014. Environmental change across a terrestrial Cretaceous-Paleogene boundary section in eastern Montana, USA, constrained by carbonate clumped isotope paleothermometry. *Geology* 42 (4), 351–354.
- Trueman, C.N., 2013. Chemical taphonomy of biomineralized tissues. *Palaeontology* 56 (3), 475–486.
- Trueman, C., Chenery, C., Eberth, D.A., Spiro, B., 2003. Diagenetic effects on the oxygen isotope composition of bones of dinosaurs and other vertebrates recovered from terrestrial and marine sediments. *J. Geol. Soc.* 160 (6), 895–901.
- Tütken, T., 2011. The diet of sauropod dinosaurs: Implications from carbon isotope analysis of teeth, bones, and plants. In: *Biology of the Sauropod Dinosaurs: Understanding the Life of Giants*, pp. 57–79.
- Tütken, T., Pfretzschner, H.U., Vennemann, T.W., Sun, G., Wang, Y.D., 2004. Paleobiology and skeletochronology of Jurassic dinosaurs: implications from the histology and oxygen isotope compositions of bones. *Palaeogeogr. Palaeoclimatol. Palaeoecol.* 206 (3–4), 217–238.
- Tütken, T., Vennemann, T.W., Pfretzschner, H.U., 2011. Nd and Sr isotope compositions in modern and fossil bones—Proxies for vertebrate provenance and taphonomy. *Geochim. Cosmochim. Acta* 75 (20), 5951–5970.
- Vonnhof, H.B., De Graaf, S., Spero, H.J., Schiebel, R., Verdegaa, S.J., Metcalfe, B., Haug, G.H., 2020. High-precision stable isotope analysis of $< 5 \mu\text{g}$ CaCO_3 samples by continuous-flow mass spectrometry. *Rapid Commun. Mass Spectrom.* 34 (19), e8878.
- Wang, Y., Cerling, T.E., 1994. A model of fossil tooth and bone diagenesis: implications for paleodiet reconstruction from stable isotopes. *Palaeogeogr. Palaeoclimatol. Palaeoecol.* 107 (3–4), 281–289.
- Wang, Y., Wang, X., Xu, Y., Zhang, C., Li, Q., Tseng, Z.J., Takeuchi, G., Deng, T., 2008. Stable isotopes in fossil mammals, fish and shells from Kunlun Pass Basin, Tibetan Plateau: paleo-climatic and paleo-elevation implications. *Earth Planet. Sci. Lett.* 270 (1–2), 73–85.
- Waskow, K., Sander, P.M., 2014. Growth record and histological variation in the dorsal ribs of *Camarasaurus* sp. (Sauropoda). *J. Vertebr. Paleontol.* 34 (4), 852–869.
- Wei, L.L., Yan, C.L., Ye, B.B., Guo, X.Y., 2008. Relationship between salinity and stable carbon isotope composition of C3 plants. *Acta Ecol. Sin.* 28 (3), 1270–1278.
- Weiner, S., Bar-Yosef, O., 1990. States of preservation of bones from prehistoric sites in the near East: a survey. *J. Archaeol. Sci.* 17 (2), 187–196.
- Woodward, H.N., Horner, J.R., Farlow, J.O., 2014. Quantification of intraskeletal histovariability in *Alligator mississippiensis* and implications for vertebrate osteohistology. *PeerJ* 2, e422.
- Wright, L.E., Schwarcz, H.P., 1996. Infrared and isotopic evidence for diagenesis of bone apatite at Dos Pilas, Guatemala: palaeodietary implications. *J. Archaeol. Sci.* 23 (6), 933–944.
- Zazzo, A., Lecuyer, C., Mariotti, A., 2004. Experimentally-controlled carbon and oxygen isotope exchange between bioapatites and water under inorganic and microbially-mediated conditions. *Geochim. Cosmochim. Acta* 68 (1), 1–12.
- Zhao, Y., Yang, Y.B., Guo, Y., Ren, G.Y., Zhang, F.C., 2021. Stable carbon isotope composition of bone hydroxylapatite: significance in paleodietary analysis. *Palaeoworld* 31 (1), 169–184.